Thermodynamics and Topology of Disordered Systems: Statistics of the Random Knot Diagrams on Finite Lattices

O. A. Vasilyev[†a] and S. K. Nechaev[†‡b]

[†] *Landau Institute of Theoretical Physics, Russian Academy of Sciences, Chernogolovka, Moscow region, 142432 Russia*

[‡] *UMR 8626, CNRS–Université Paris XI, LPTMS, Université Paris Sud, 91405 Orsay Cedex, France*

(Journal of Experimental and Theoretical Physics, **93** (2001), 1119–1136)

The statistical properties of random lattice knots, the topology of which is determined by the algebraic topological Jones-Kauffman invariants has been studied by analytical and numerical methods. The Kauffman polynomial invariant of a random knot diagram has been represented by a partition function of the Potts model with a random configuration of ferro- and antiferromagnetic bonds, which allowed the probability distribution of the random dense knots on a flat square lattice over topological classes to be studied. A topological class is characterized by the highest power of the Kauffman polynomial invariant and interpreted as the free energy of a q–component Potts spin system for $q \to \infty$. It is shown that the highest power of the Kauffman invariant is correlated with the minimum energy of the corresponding Potts spin system. The probability of the lattice knot distribution over topological classes was studied by the method of transfer matrices, depending on the type of local crossings and the size of the flat knot diagram. The obtained results are compared to the probability distribution of the minimum energy of a Potts system with random ferro- and antiferromagnetic bonds.

[a] E-mail: vasilyev@itp.ac.ru

[b] E-mail: nechaev@ipno.in2p3.fr

Contents

I. INTRODUCTION

New interesting problems are formulated, as a rule, in the boundary regions between traditional fields. This is clearly illustrated by the statistical physics of macromolecules, which arose due to the interpenetration of the solid state physics, statistical physics, and biophysics. Another example of a new, currently forming field is offered by the statistical topology born due to merging of the statistical physics, theory of integrable systems, algebraic topology, and group theory. The scope of the statistical topology includes, on the one hand, mathematical problems involved in the construction of topological invariants of knots and links based on some solvable models and, on the other hand, the physical problems related to determination of the entropy of random knots and links. In what follows, we pay attention predominantly to problems of the latter kind that can be rather conventionally separated into a subfield of "probabilistic-topological" problems [1]. Let us dwell on this class of problems in more detail.

Consider a lattice embedded into a three-dimensional space, for which Ω is the ensemble of all possible closed self-nonintersecting trajectories of N steps with a fixed point. Let ω denote some particular realization of such a trajectory. The task is to calculate the probability P for a knot of specific topological class for all trajectories $\omega \in \Omega$. This can be formally expressed as

$$P\{\mathrm{Inv}\} = \frac{1}{\mathcal{N}(\Omega)} \sum_{\{\omega\in\Omega\}} \delta\Big\{\mathrm{Inv}(\omega) - \mathrm{Inv}\Big\} \tag{1}$$

where $\mathrm{Inv}(\omega)$ is a functional representation of the invariant for a knot on trajectory ω, Inv is a particular topological invariant characterizing the given topological type of the knot or link, $\mathcal{N}(\Omega)$ is the total number of trajectories, and δ is the delta function. The probability under consideration should obey the usual normalization condition $\sum\limits_{\{\mathrm{Inv}\}} P\{\mathrm{Inv}\} = 1$. The entropy S of a knot of the given topological type is defined as

$$S\{\mathrm{Inv}\} = \ln P\{\mathrm{Inv}\} \tag{2}$$

Based on the above definitions, it is easy to note that the probabilistic–topological problems are similar to those encountered in the physics of disordered systems and sometimes, as demonstrated below, of the thermodynamics of spin glasses. Indeed, the topological state plays the role of a "quenched disorder" and the functional $P\{\mathrm{Inv}\}$ is averaged over the trajectory fluctuations at a fixed "quenched topological state", which is similar to calculation of a partition function for a spin system with "quenched disorder" in the coupling constant. In the context of this analogy, a question arises as to whether the concepts and methods developed over many years of investigation into the class of disordered statistical systems can be transferred to the class of probabilistic-topological problems, in particular, whether the concept of *self-averaging* is applicable to the knot entropy S.

The main difference between the systems with topological disorder and the standard spin systems with disorder in the coupling constant is a strongly nonlocal character in the first case: a topological state is determined only for the entire closed chain, is a "global" property of this chain, and is difficult to determine it for any arbitrary subsystem. Therefore, we may speak of the topology of a part of some closed chain only in a very rough approximation. Nevertheless, below we consider a lattice model featuring a unique relationship between the topological disorder and the disorder in the local coupling constant for a certain disordered spin system on the lattice.

Every time when we deal with topological problems, there arises the task of classification of the topological states. A traditional topological invariant, known as the Gauss invariant, in inapplicable because this Abelian (commutative) characteristic takes into account only a cumulative effect of the entanglement, not reflecting the fact that the topological state depends significantly on the sequence in which a given entanglement was formed. For example, when some trial trajectory entangles with two (or more) obstacles, there may appear configurations linked with several obstacles simultaneously, while being not linked to any one of these obstacles separately. In this context, it is clear that most evident questions concerning calculation of the probability of a knot formation as a result of the random closing of the ends of a given trajectory cannot be solved in terms of the Gauss invariant because this characteristic is incomplete.

A very useful method of the classification of knots was offered by a polynomial invariant introduced by Alexander in 1928. A breakthrough in this field took place in 1975-1976, when it was suggested to use the Alexander invariants for classification of the topological state of a closed random trajectory computer-simulated by the Monte Carlo method. The results of these investigations showed that the Alexander polynomials, being a much stronger invariants compared to the Gauss integral, offer a convenient approach to the numerical

investigation of the thermodynamic characteristics of random walks with topological constraints. The statistical-topological approach developed in [2] has proved to be very fruitful: the main results gained by now were obtained using this method with subsequent modifications.

An alternative polynomial invariant for knots and links was suggested by Jones in [3,4]. This invariant was defined based on the investigation of the topological properties of braids [5,6]. Jones succeeded in finding a profound connection between the braid group relationships and the Yang-Baxter equations representing a necessary condition for commutativity of the transfer matrix [7]. It should be noted that neither the Alexander, Jones, and HOMFLY invariants, nor their various generalizations are complete. Nevertheless, these invariants are successfully employed in solving statistical problems. A clear geometric meaning of the Alexander and Jones invariants was provided by the results of Kauffman, who demonstrated that the Jones invariants are related to a partition function of the Potts spin model [9]. Later Kauffman and Saleur showed that the Alexander invariants can be represented by a partition function in the free fermion model [10].

We employed the analogy between the Jones-Kauffman polynomial invariant and the partition function in the Potts model with ferro (f-) and antiferromagnetic (a-) links [11,12] to study the statistical properties of knots. In particular, the method of transfer matrices developed in [13–15] was used to determine the probability $P\{f_K\}$ of finding a randomly generated knot K in a particular topological state characterized by the invariant f_K.

The idea of estimating $P\{f_K\}$ is briefly as follows: (i) the Jones-Kauffman invariant is represented as a partition function of the Potts model with disorder in the coupling constant; (ii) the thermodynamic characteristic of the ensemble of knots are calculated using the method of transfer matrices for the Potts spin system.

The paper is arranged as follows. Section 2 describes the model, defines the Jones-Kauffman polynomial invariant, and shows a connection of this invariant to the Potts model. Section 3 presents the numerical methods employed and introduces the necessary supplementary constructions. The results of numerical modeling are discussed and the conclusions are formulated in Section 4.

II. KNOTS ON LATTICES: MODEL AND DEFINITIONS

Consider an ensemble of randomly generated dense knots on a lattice in a three-dimensional space. A knot is called "dense" if the string forming this knot is tightly fit to the lattice, not fluctuating in the space. In this case, the knots of various topological types possess no configuration entropy and the probability of formation of a knot belonging to a given topological type is determined only by a local topology of the system.

Not taking into account the fluctuational degrees of freedom of the lattice sites, this model is obviously very simplified. Nevertheless, this approach adequately reflects a physical situation, for example, in the statistical physics of condensed (globular) state of polymer macromolecules. Virtually all presently existing models taking into account topological restrictions with respect to the admissible spatial configurations of polymer chains assume a small density of the polymer, that is, describe a situation far from the compact state of globules. A hypothesis of the essentially new globular phase of a ring knotless macromolecule (crumpled globule) existing at a large polymer density (i.e., in the state of dense knots) was

formulated in [16]. Despite an indirect experimental evidence for validity of the crumpled globule hypothesis [17], direct observation of such objects in real experiments or computer simulations encounters considerable technical difficulties. In this context, investigation of the distribution of randomly generated dense knots of various topological types may provide for a better understanding of the structure of the phase space of knotted polymers in the globular state.

Analysis of a string configuration in the three-dimensional space is not very convenient for determining the topological type of a knot. The standard method consists in projecting the knot onto a plane in the general position (with no more than two knot segments intersecting at each point of the plane) and determining which segment line passes above (overcrossing) or below (undercrossing) in accordance with the knot topology. Such a projection, featuring over- and under-crossing, is called the diagram of a knot. In what follows we deal only with statistics of the knot diagrams. Evidently, this description implies an additional simplification of the model, but we believe that (in the phase of dense knots under consideration) the additional restrictions are not very significant since, as noted above, the knot entropy contains no contribution due to the string fluctuations.

Thus, let us consider a square lattice of the size $N = L \times L$ on a plane, which is rotated for convenience by the $\pi/4$ angle. The lattice is filled by a (dense) trajectory featuring intersections at each lattice site with clear indications of the threads passing above and below (see an example of the 3×3 lattice in Fig.1a). As can be readily verified, a dense trajectory on a lattice with an odd L is unique, that is, represents a knot with the topology unambiguously determined by the pattern of over- and undercrossing and the boundary conditions. In this case, the probability of realization of the knot belonging to a given topological type is determined by the distribution of over- and undercrossing in all lattice sites. The problem considered in this study is to describe the distribution of dense knots over topological classes for various kinds of the over- and undercrossing distributions.

A. Reidemeister moves and definition of the kauffman invariant

In solving any topological problem, the main point consists in comparing the knots. A knot diagram on the plane obey the following Reidemeister theorem [18]:*Two knots in the tree-dimensional space can be continuously transformed into each other if and only if the diagram of one knot can be transformed into that of the other knot by a sequence of local transformations (moves) of types I, II, and III* (see Fig.2).

As can be seen in Fig.2, the Reidemeister move I leads to the formation of a singularity on the plane during continuous fastening of the loop; this move is forbidden for smooth trajectories on the plane. Two knots are called regularly isotopic if their plane diagrams can be transformed into each other by means of the Reidemeister moves II and III. When the mutual transformation of the knot diagrams requires using the Reidemeister moves of all three types, the knots are called ambiently isotopic.

Consider a two-dimensional knot diagram as a graph in which all intersection points (vertices) are characterized by the order of crossing (over- and under-crossing). Then each intersection point belongs to one of the two possible crossing modes. Let a kth point of the graph be characterized by the variable ϵ_k acquiring the values ± 1, depending on the mode of crossing.

Let us define the algebraic Kauffman invariant as a sum over all possible variants of splitting the diagram at the vertices. According to this, each splitting is ascribed a certain statistical weight by the following rule: a vertex with $\epsilon = +1$ is given the weight A or B corresponding to the horizontal or vertical splittings, respectively; for a vertex with $\epsilon = -1$, the weight B corresponds to the horizontal splitting and the weight A, to the vertical splitting. This definition can be illustrated by the following scheme:

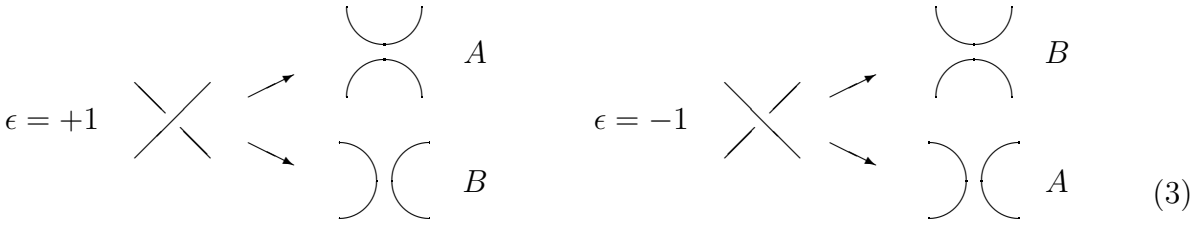

(3)

Thus, there are 2^N various microstates for the diagram of a knot possessing N vertices. Each state ω of the knot diagram represents a set of nonintersecting and self-nonintersectiong cycles. The manifold of all microstates is denoted by $\{\omega\}$ (below, the braces $\{\ldots\}$ will denote summing over these states). Let $S(\omega)$ be the number of cycles for the microstate ω. Consider a partition function

$$f_{KR} = \sum_{\{\omega\}} d^{S(\omega)-1} A^{l(\omega)} B^{N-l(\omega)} \tag{4}$$

where the sum is taken over all 2^N possible splittings of the diagram; $l(\omega)$ and $N - l(\omega)$ are the numbers of vertices with the weights A and B, respectively, for a given set of splittings of the microstate ω. Kauffman derived the following statement [9]: a polynomial f_{KR} of the variables A, B, and d representing a partition function (4) is a topological invariant of the regularly isotopic knots, if and only if the parameters A, B, and d obey the relationships: $AB = 1$ and $ABd + A^2 + B^2 = 0$. A proof of this statement in [9] is based on verification of the invariance of the partition function f_{KR} with respect to the Reidemeister moves II and III. (The invariant for all tree Reidemeister moves is defined below.) The latter relationships pose the following restrictions on the parameters A, B, and d in Eq. (4):

$$\begin{aligned} B &= A^{-1}, \\ d &= -A^2 - A^{-2} \end{aligned} \tag{5}$$

which imply that invariant (4) is a polynomial of the single variable A.

B. A partition function of the Potts model as a bichromatic polynomial

Consider an arbitrary flat graph containing N vertices. Let ith vertex be characterized by a spin variable σ_i $(1 \leq \sigma_i \leq q)$ and each edge of the graph, connect ing the ith and jth spins $(1 \leq \{i, j\} \leq N)$, by the coupling constant $J_{i,j}$. The energy of the Potts model is defied as [7]

$$E = -\sum_{\{i,j\}} J_{i,j} \delta(\sigma_i, \sigma_j)$$

where the sum over $\{i,j\}$ is taken only for the adjacent spins connected by edges of the graph. Then, the partition function can be expressed as

$$Z = \sum_{\{\sigma\}} \exp\left(\sum_{\{i,j\}} \frac{J_{i,j}}{T}\delta(\sigma_i,\sigma_j)\right)$$

where $\{\}$ denotes summation over all possible spin states, and the sum over $\{i,j\}$ is taken as indicated above. The last expression can be written in the following form:

$$Z = \sum_{\{\sigma\}} \prod_{\{i,j\}} \left(1 + v_{i,j}\delta(\sigma_i,\sigma_j)\right), \quad v_{i,j} = \exp\left(\frac{J_{i,j}}{T}\right) - 1 \tag{6}$$

A pair of adjacent spins i and j introduces into the product term a contribution equal to $\exp(\frac{J_{i,j}}{T})$ for $\sigma_i = \sigma_j$ and a unity contribution for $\sigma_i \neq \sigma_j$. Let us perform a procedure according to the following rules to a given spin configuration and the corresponding graph:

- an edge is removed from the graph if a contribution to the above product from the spins connected by this edge is unity;
- an edge is retained in the graph if the contribution from the spins σ_i and σ_j connected by this edge is $\exp(\frac{J_{i,j}}{T})$. This procedure ensures a one-to-one mapping between the spin configuration corresponding to a product term in the sum (6) and the related set of graph components.

Consider a graph G containing M edges and C connected components (an isolated vertex is considered as a separate component). Upon summing over all possible spin configurations and the corresponding subdivisions of the graph G, we may present the sum (6) in the following form:

$$Z = \sum_{\{G\}} q^C \prod_{\{i,j\}}^{M} v_{i,j} \tag{7}$$

where $\{G\}$ denotes summing over all graphs and $\prod_{\{i,j\}}^{M}$ is the product over all edges of the graph G. Note that expression (7) can be considered as an analytic continuation of the Potts spin system to non-integer and even complex q values.

For $v_{i,j} \equiv v$, expression (7) coincides with a well-known representation of the partition function of the Potts model in the form of a bichromatic polynomial (see, e.g., [7,19])). The same expression is involved in the correspondence between the Potts model and the model of correlated percolation over sites and bonds suggested by Fortuin and Kastelleyn [20], which serves a base for the Monte Carlo cluster algorithms developed by Swedsen and Wang [21] and Wolff [22] for the Potts model.

C. Kauffman invariant represented as a partition function for the Potts model

The Kauffman invariant of a given knot can be represented as a partition function for the Potts model on a graph corresponding to an arbitrary plane diagram of this knot, but we restrict the consideration below to an analysis of the knots on lattices.

Let us rewrite the Kauffman invariant in the form of a partition function for the Potts model determined in the preceding section, with M denoting the lattice knot diagram (see Fig.1a). The auxiliary variables $s_k = \pm 1$ describe the mode of the knot splitting in each kth lattice site, irrespective of the values of variables $\epsilon_k = \pm 1$ in the same vertices:

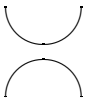

$s_k = +1$

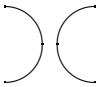

$s_k = -1$

Let $\omega = \{s_1, s_2, \ldots, s_N\}$ be the set of all variables characterizing the mode of splitting in the lattice containing N intersections. The Kauffman invariant (4) can be written in the following form:

$$f_{KR}(\epsilon_1, ..., \epsilon_N) = \sum_{\{\omega\}} (-A^2 - A^{-2})^{S(\omega)-1} \exp\left(\ln A \sum_{k=1}^{N} \epsilon_k s_k\right) \tag{8}$$

Here, $\{\omega\}$ indicates summing over all values of the variables s_k (i.e. over all modes of splitting thy lattice diagram M) and the variables ϵ_k characterize a particular realization of "quenched" disorder in the system. Now we can demonstrate that configurations obtained as a result of splitting the diagram are in a one-to-one correspondence to configurations of the Potts model on a dual lattice.

Consider the Potts model lattice Λ corresponding to the lattice M (see Fig.1b) , where open circles indicate positions of the Potts spins). The $b_{i,j}$ edge of lattice Λ corresponds to the kth site of the lattice diagram M. Therefore, disorder in the vertices of diagram M set by the variables ϵ_k coincides with the disorder in edges $b_{i,j}$ of the lattice Λ, that is, with the disorder in coupling constants. Let us define the disorder of $b_{i,j}$ for the lattice Λ via the coupling constants at the corresponding kth site of the lattice diagram M:

$$b_{i,j} = \begin{cases} -\epsilon_k, & \text{if the bond } (i,j) \text{ is vertical} \\ \epsilon_k, & \text{if the bond } (i,j) \text{ is horizontal} \end{cases} \tag{9}$$

It should be recalled that the definition of the Kauffman invariant (4) is based on splitting the lattice diagram M into polygons representing a system of closed densely packed nonintersecting contours (Fig.1b). For a given configuration of splitting the lattice diagram M and the corresponding dual lattice Λ, we take the following agreement: all edges of the lattice Λ not crossed by polygons of the lattice M are labeled. In Fig.1b, the labeled edges are indicated by dashed lines. All the remaining edges of Λ are unlabeled. In these terms, the exponent in the partition function in Eq. (8) can be written as follows:

$$\begin{aligned} \sum_k s_k\epsilon_k = \sum_{\text{mark}} s_k\epsilon_k + \sum_{\text{nonmark}} s_k\epsilon_k = \sum_{\text{mark}}^{\text{hor.}} s_k\epsilon_k + \sum_{\text{mark}}^{\text{ver.}} s_k\epsilon_k + \sum_{\text{nonmark}}^{\text{hor.}} s_k\epsilon_k + \sum_{\text{nonmark}}^{\text{ver.}} s_k\epsilon_k = \\ \sum_{\text{mark}}^{\text{hor.}} b_{i,j} + \sum_{\text{mark}}^{\text{ver.}} b_{i,j} - \sum_{\text{nonmark}}^{\text{hor.}} b_{i,j} - \sum_{\text{nonmark}}^{\text{ver.}} b_{i,j} = -\sum_{\text{all}} b_{i,j} + 2\sum_{\text{mark}} b_{i,j} \end{aligned} \tag{10}$$

where

$$\sum_{\text{mark}} b_{i,j} + \sum_{\text{nonmark}} b_{i,j} = \sum_{\text{all}} b_{i,j}$$

Let m_ω be the number of labeled edges and C_ω be the number of connected components in the labeled graph ω with N_p vertices (each vertex corresponding to a Potts spin). The Euler relationship for this graph is

$$S(\omega) = 2C_\omega + m_\omega - N_p$$

Now we can readily transform Eq. (8) to

$$f_{KR}(A, \{b_{i,j}\}) = (-A^2 - A^{-2})^{-(N_p+1)} \prod_{\text{all}}^{N} \left(A^{-b_{i,j}}\right) \sum_{\{G\}} \left(-A^2 - A^{-2}\right)^{2C_\omega} \prod_{\text{mark}}^{m_\omega} \left(A^{2b_{k,l}} \left(-A^2 - A^{-2}\right)\right) \tag{11}$$

by using (10) and the fact that N is odd. Comparing expressions (11) and (6), we obtain the equality

$$\sum_{\{G\}} \left(A^2 + A^{-2}\right)^{2C_\omega} \prod_{\text{mark}}^{m_\omega} \left(A^{2b_{i,j}} \left(-A^2 - A^{-2}\right)\right) \equiv \sum_{\sigma} \prod_{\{i,j\}} \left(1 + v_{i,j}\delta(\sigma_i, \sigma_j)\right) \tag{12}$$

in which the right-hand part coincides with a partition function of the Potts model represented in the form of a bichromatic polynomial. From this we obtain

$$v_{i,j} = A^{2b_{i,j}} \left(-A^2 - A^{-2}\right) = -1 - A^{4b_{i,j}}$$
$$q = (A^2 + A^{-2})^2$$

Since the disorder constants may acquire only discrete values $b_{i,j} = \pm 1$, we may write the following expression for the coupling constants $J_{i,j}$:

$$J_{i,j} = T \ln\left(1 - \left(A^2 + A^{-2}\right) A^{2b_{i,j}}\right) = T \ln\left(-A^{4b_{i,j}}\right) \tag{13}$$

Thus, we arrive at the following statement. The topological Kauffman invariant $f_{KR}(A)$ of the regularly isotopic knots on the lattice M can be represented in the form of a partition function for a two-dimensional Potts model on the corresponding dual lattice Λ:

$$f_{KR}(A, \{b_{i,j}\}) = K\left(A, \{b_{i,j}\}\right) \, Z\left(q(A), \{J_{i,j}(b_{i,j}, A)\}\right) \tag{14}$$

where

$$K\left(A, \{b_{i,j}\}\right) = \left(A^2 + A^{-2}\right)^{-(N_p+1)} \exp\left(-\ln A \sum_{\{i,j\}} b_{i,j}\right) \tag{15}$$

is a trivial factor independent of the Potts spins. Here, the partition function of the Potts model is

$$Z\left(q(A), \{J_{i,j}(b_{i,j}, A)\}\right) = \sum_{\{\sigma\}} \exp\left(\sum_{\{i,j\}} \frac{J_{i,j}(b_{i,j}, A)}{T} \delta(\sigma_i, \sigma_j)\right) \tag{16}$$

with the coupling constant $J_{i,j}$ and the number of states q given by the formulas

$$\frac{J_{i,j}}{T} = \ln(-A^{4b_{i,j}}), \qquad q = (A^2 + A^{-2})^2 \tag{17}$$

and the variable $b_{i,j}$ expressing disorder on edges of the lattice Λ corresponding to the lattice M. A relationship between $b_{i,j}$ and ϵ_k is defined in Eq. (9).

A specific feature of the partition function (16) is the existence of a relationship between the temperature T and the number of spin states q. For this reason, T and q cannot be considered as independent variables. Once a positive q value is fixed, the variable A can formally acquire the complex values according to Eqs. (17), where logarithm can be taken of a complex argument. The appearance of complex quantities in the partition function can be interpreted in two ways. On the one hand, this implies expansion of the domain of the partition function to the complex plane. On the other hand, the parameters T and $J_{i,j}$ do not enter explicitly into an expression for the Kauffman invariant and, hence, their complex values do not require any special consideration. Below we will be interested mostly in the probability distribution of the maximum power in the polynomial invariant and, therefore, can digress from particular values of the variables A, T, and $J_{i,j}$.

Thus, we have determined an invariant f_{KR} for the regularly isotopic knots, the diagrams of which are invariant with respect to Reidemeister moves II and II. In order to obtain an invariant f_{KR} for the ambiently isotopic knots with oriented diagram, the corresponding partition function has to be invariant with respect to the Reidemeister moves of all types. Let us characterize each oriented intersection by a variable $c_k = \pm 1$ according to the following rule

(a)  $c_k = -1$ (b)  $c_k = +1$

In addition, we define the knot twisting $Tw(\omega)$ as a sum of the $c_k = b_k$ values taken over all intersections: $Tw(\omega) = \sum\limits_k c_k$ The invariant $f_{KI}(\omega)$ of the ambiently isotopic knots can be expressed as follows [9]:

$$f_{KI}(\omega) = f_{KR}(\omega)(-A)^{3Tw(\omega)} \tag{18}$$

It should be noted that our boundary conditions imply that $c_k = b_k$. As is known, the Kauffman polynomial invariant $f_{KI}(\omega; A)$ of the ambiently isotopic knots as a function of variable A is equivalent to the Jones polynomial invariant $f_J(\omega; x)$ of the variable $x = A^4$. Now we can use formulas (14) and (15) to express the Jones invariant through a partition function of the Potts model. Let a partition function of the Potts model have the form $Z(t; q) = \sum\limits_E H(E, q)t^{-E}$ where $t = e^E$; E denotes the energy levels over which the sum is taken, and $H(E, q)$ is the degree of degeneracy of an energy level E for a given q value. Taking into account that $x = A^4 = -t$ and using formulas (14), (15) and (18), we obtain the following expression for the Jones polynomial invariant:

$$f_J = \sum_E H(E; q = 2 + x + x^{-1})(-x)^{-E}(1 + x)^{-N_p-1}(-\sqrt{x})^{N_p+1+\sum\limits_{\{i,j\}} b_{i,j}} \tag{19}$$

In what follows, by the maximum power of a polynomial invariant we imply the maximum power of variable x in the Jones polynomial invariant f_J. It will be born in mind that the power of the Kauffman polynomial invariant f_{KI} of the ambiently isotopic knots is obtained from the corresponding power of the Jones polynomial invariant through simply multiplying by a factor of four.

As indicated above, out task is to calculate the probability $P\{f_J\}$ of finding a knot on a lattice in the topological state with a preset J ones-Kauffman invariant $f_J(x,\{\epsilon_k\})$ among all the 2^N possible disorder realizations $\{\epsilon_k\},\ k=1,\ldots,N$ This probability can formally be written as

$$P_N\{f_J\}=\frac{1}{2^N}\sum_{\{\epsilon_k\}}\delta\Big(f_J(x,\{\epsilon_1,\ldots,\epsilon_N\})-f_J\Big)$$

Thus, the topological disorder determined by a random independent selection of intersections of the $\epsilon=+1$ and $\epsilon=-1$ types represents a random quenched external field. When we use the Jones invariant, each topological class (homotopic type) is characterized by a polynomial. In this case, precise identification of the homotopic type for a knot on a lattice containing N intersections will require N variables. Since the number of various homotopic types increases as 2^N , it is very difficult to study the probability of each separate homotopic type characterized by N variables. For this reason, we introduce a simplified characteristic of a knot on a lattice - the maximum power n of the polynomial invariant $f_J(x)$:

$$n=\lim_{|x|\to\infty}\frac{\ln f_J(x)}{\ln(x)} \tag{20}$$

For a trivial knot $n=0$ and, as the knot complexity grows, the maximum power increases (not exceeding N). Thus, ensemble of all of knots on a lattice can be divided into subclasses characterized by the power n $(0\le n\le N)$ of the Jones polynomial invariant. In these terms, we will study the probability that a randomly selected knot belongs to one of these subclasses (and is characterized by the maximum power n of the Jones invariant). Random knots can be generated by two methods:

1. place a fixed number of intersections with $\epsilon=-1$ on the knot diagram with N vertices (accordingly, the other vertices belong to intersections of the $\epsilon=+1$ type);

2. place intersections of the $\epsilon=-1$ and $\epsilon_k=-1$ types in each vertex with the probabilities p and $1-p$, respectively.

As can be readily seen, a trivial knot having all intersections of the $\epsilon=+1$ type corresponds to a partition function with the ferro (f-) and antiferromagmetic (a-) bonds distributed in accordance with the rule (9). An impurity (corresponding to $\epsilon_k=-1$ of the knot diagram) will be considered as a change in the sign of $b_{i,j}$ relative to the values characterizing trivial knots. Note that we must differentiate between the notion of impurity (a change in the sign of $b_{i,j}$) from the a-bond with $b_{i,j}=-1$. For a trivial knot with all $\epsilon_k=1$, the lattice contains no impurities while containing the a-bonds.

III. AUXILIARY CONSTRUCTIONS AND NUMERICAL METHODS

A. The form of a lattice for the Potts model and the positions of ferro- and antiferromagnetic bonds

Now we describe the geometry of a lattice for the Potts model corresponding to a knot diagram of the $N=L\times L$ size. This study is restricted to square lattices, although all

considerations remain valid for rectangular lattices as well. Figure 3a shows an example of the trivial knot on a lattice with $N = 5\times5$. Positions of the Potts spins corresponding to this lattice diagram are indicated by circles. The Potts spin lattice corresponding to this knot is depicted in Fig.3b, where the f-bonds (that would be horizontal in Fig.1) are indicated by solid lines and the a-bonds (that would be vertical in Fig.1) are indicated by dashed lines. In Fig.3c, the same lattice is transformed into a rectangular one of the $L_h \times L_v$ type, where $L_h = L + 1$ and $L_v = (L + 1)/2$ (in this particular case, $L_v = 3$, $\quad L_h = 6$. The partition function of the Potts model is studied below for a rectangular lattice of this type.

The fact that the height of the lattice for the Potts model is half that of the lattice knot diagram (see Figs.3a–c) is very convenient in the case of using the method of transfer matrices, where the computational time expenditure exponentially depends on the lattice height. Let $N = L \times L$ be the total number of bonds in the lattice, with $N_+ = \sum\limits_{\{i,j\}} \delta(b_{i,j}, 1)$ representing the number of f-bonds and $N_- = \sum\limits_{\{i,j\}} \delta(b_{i,j}, -1)$ the number of a-bonds. An impurity, corresponding to $\epsilon_k = -1$ in the initial lattice, is described by a change in sign of the corresponding constant $b_{i,j}$ for the Potts model lattice.

It should be emphasized once again that by impurity we imply a change in the type of intersection from $\epsilon_k = +1$ to $\epsilon_k = -1$, which corresponds to a change in sign of the coupling constant $b_{i,j}$ for this intersection, rather than to the a-bond (such bonds are present in the Potts model lattice of the trivial knot). A trivial knot is characterized by the absence of impurities on the Potts model lattice $N_+ = \frac{N+1}{2}$, $N_- = \frac{N-1}{2}$ Note that the Kauffman invariants for a knot and its mirror image are different. This is due to the following property of the Jones invariant: the invariant of the mirror image of a knot is obtained by substituting $t \to t^{-1}$ (and $A \to A^{-1}$), after which the distribution of powers in the polynomial is asymmetric with respect to the substitution $p \to 1 - p$.

B. The method of transfer matrix

It should be recalled that we are interested in determining the probability distribution of the maximum power n (averaged over various types of intersections in the knot diagram) of the Jones-Kauffman invariant. According to definition (20), the coefficient at the term of the maximum power n in the Jones polynomial of a randomly generated knot is insignificant. Let us fix a certain value n_0, generate an ensemble of random knot diagrams, and determine the fraction of knots the polynomials of which contain the maximum power $n = n_0$.

The traditional approach to numerical analysis of a q-component Potts spin system assumes that each possible state of the column L_v spins corresponds to an eigenvector of the q^{L_v}-dimensional transfer matrix. With computers of the P-II-300 type and a reasonable computational time, the maximum possible size of the transfer matrix is 100-200. This corresponds to a spin strip width $L_v = 8$ for $q = 2$ and $L_v = 4$ for $q = 3$. Obviously, this method cannot be used for investigation of the Potts model with large q values.

A method of transfer matrices applicable to the case of arbitrary q was developed by Blöte and Nightingale [13]. The basic idea of this method is that each eigenvector corresponds to a subdivision of the column into clusters of "coupled" spins. By definition, the spins in each cluster are parallel. Therefore, the number of "colors" q can be considered simply as a parameter taking any values (including non-integer and even complex). A detailed

description of this method can be also found in [14,15], where this approach was used to study the Potts model with impurities on the bonds and to determine the roots of a partition function for the Potts model in the complex plane.

Below we will briefly describe the principles of determining a basis set in the space of coupled spins and constructing transfer matrices in this basis. This description follows the results reported in [15].

A basis set corresponds to a set of various subdivisions of the spin column into clusters of coupled spins. We must take into account that the subdivision should admit realization in the form of a flat graph on a half-plane. Now we can describe a recursive procedure for determining the basis set. Let a basis set be available for a column with the height L_v. Upon adding one more spin from below, we obtain a column with the height $\tilde{L}_v$. Then we take, for example, a subdivision $v_1(L_v)$ corresponding to the first basis vector L_v and begin to generate subdivisions corresponding to the basis vectors for the column $\tilde{L}_v$ by attaching the added spin to those existing in $v_2(L_v)$. In each step, we check for the possibility of attaching this spin within the framework of the flat graph on a half-plane. after the attempt at attaching the added spin to all existing clusters, we generate a subdivision in which the added cluster is separate. Then we take the next subdivision (for example, $v_2(L_v)$) for the L_v column and repeat the generation procedure.

The procedure begins with a single spin as depicted in Fig.4. This spin is assigned the index of unity as belonging to the first cluster. Then another spin is added from below to the same column. Accordingly, the strip of two spins may occur in one of the two states: $v_1(L_v = 2)$, in which the spins are coupled and belong to cluster 1, or $v_2(L_v = 2)$, in which the spins are not coupled and belong to clusters 1 and 2 (Fig.4). A basis set for the strip of three spins is obtained by adding another spin from below and coupling this spin to all clusters. The clusters are enumerated by integers top to bottom, while vectors in the basis set are enumerated in the order of generation. As can be readily seen, the first basis vector corresponds to a state in which all spins are coupled to each other and belong to the same cluster, while the last basis vector corresponds to the state where all spins are uncoupled and the number of clusters equals to the number of spins in the column. The total number of vectors in the basis set for a strip of m spins is determined as the Catalan number $C_m = \frac{1}{m+1}\binom{2m}{m}$ with the corresponding index number (see [15]).

Let us denote by $v_i(\backslash k)$ a subdivision obtained upon separating the kth spin from the subdivision v_i to form a separate cluster; $v_i(\{k,l\})$ will denote a subdivision in which the clusters containing kth and lth spins are combined to form a common cluster. Following a method described in [15], let us form the matrix

$$D_{i,j}(k) = \delta(v_j(\backslash k), v_i) + q\delta(v_j(\backslash k), v_j)$$

As can be seen, an element of the matrix $D_{i,j}(k)$ is non-zero if the kth spin is not coupled to any other spin in the subdivision v_i. When the same spin is not coupled to any other in the jth subdivision as well, the matrix element is q, otherwise it is taken equal to unity. We will also introduce the matrix $C(k,l)$ defined as

$$C_{i,j}(k,l) = \delta(v_j(\{k,l\}), v_i)$$

the elements of which are equal to unity if and only if the subdivision v_i is obtained from the subdivision v_j by combining clusters containing the kth and lth spins.

Now let us consider a lattice structure with the first two rows such as depicted in Fig.5d (for an even index $j+1$ in the second column) and Fig.5e (for an odd index $j+1$ in the second column). The spin columns are enumerated by index j: $1 \leq j \leq L_h$, while the spin position in a column is determined by index i: $1 \leq i \leq L_v$.

According to these constructions, the transfer matrices of the type $T^{even}(j+1=2k)$, which corresponds to adding an even column $j+1=2k$ after an odd one $j=2k-1$ (we add the columns from the right-hand side), contain bonds between the spins $\sigma_{i,j=2k-1}$ and $\sigma_{i+1,j=2k}$. The transfer matrices of the type $T^{odd}(2j+1)$, which corresponds to adding an odd column $j+1=2k+1$ after an even one $j=2k$, contain bonds between the spins $\sigma_{i,j=2k}$ and $\sigma_{i-1,j+1=2k+1}$.

Let the contribution to a statistical weight corresponding to the f-bond $b(\sigma_{i,j},\sigma_{i',j'})=1$ be expressed as

$$t=\exp(\beta J)$$

where $\beta=\frac{1}{T}$. Then the a-impurity $b(\sigma_{i,j},\sigma_{i',j'})=-1$ corresponds to the weight

$$t^{-1}=\exp(-\beta J)$$

and the total contribution of a given configuration to the statistical weight of the system is $t^{b(\sigma_{i,j},\sigma_{i',j'})}$. Let us define a matrix for the horizontal bond $(\sigma_{i,j},\sigma_{i,j+1})$ as

$$P(i,j)=I(t^{b(\sigma_{i,j},\sigma_{i,j+1})}-1)+D(i,j)$$

and the matrices for "sloped" bonds as

$$\begin{array}{l} R^{even}(i,j)=I+C(i,j)(t^{b(\sigma_{i,j},\sigma_{i+1,j+1})}-1) \\ R^{odd}(i,j)=I+C(i,j)(t^{b(\sigma_{i,j},\sigma_{i-1,j+1})}-1) \end{array}$$

where I is the unit matrix.

Then the transfer matrices can be expressed as follows:

$$\begin{array}{rcl} T^{even}(j) & = & P(L_v,j)R^{even}(L_v-1,j)P(L_v-1,j)\ldots R^{even}(1,j)P(1,j) \\ T^{odd}(j) & = & P(1,j)R^{odd}(2,j)P(2,j)\ldots R^{odd}(L_v,j)P(L_v,j) \end{array}$$

and the partition function is

$$Z(t)=u^T\prod_{k=1}^{L_h/2-1}T^{even}(L_h)\left(T^{odd}(2k+1)T^{even}(2k)\right)v_{max}$$

where v_{max} is a basis vector with the maximum number corresponding in our representation to the state in which all spins belong to different clusters and $u^\top=\{q^{N_{CL}(v_1)},q^{N_{CL}(v_2)},...,q^{N_{CL}(v_{max})}\}$ so that $u^\top v_i=q^{N_{CL}(v_i)}$, where $N_{CL}(v_i)$ is the number of various clusters in the subdivision v_i. For the first basis vector, $N_{CL}(v_1)=1$ (a single cluster) and the last vector corresponds to $N_{CL}(v_{max})=L_v$ – L_v different clusters.

The general algorithm of the calculation is as follows.

1. Generate basis set vectors for a spin strip of the required width;

2. Use this basis set to generate the matrices $R(i,j)$, $P(i,j)$ in cases of f- and a-bonds (σ_i,σ_j)

3. Generate a distribution of impurities on the lattice using a random number generator;

4. Generate the transfer matrices for the Potts spin model and the polynomial invariant;

5. Calculate a partition function for the Potts model, the polynomial invariant, the minimum energy, and the maximum power of the polynomial.

6. Repeat points 3-5 and perform averaging over various realizations of the distribution of impurities on the lattice.

The error was determined upon averaging over ten various series of calculations. For each realization of the impurity distribution, the program simultaneously determines both the polynomial invariant and the partition function of the Potts model for an arbitrary (but fixed) q value. This method allows us to study correlations between the maximum power of the polynomial and the minimum energy within the framework of the Potts model on the corresponding lattice.

IV. RESULTS OF CALCULATIONS

A. Correlations between the maximum power of Jones polynomial of the lattice knot and the minimum energy of the Potts model

Let us consider dependence of the maximum power of the Jones polynomial on the type of the partition function for the Potts model. Formula (19) explicitly relating the Jones-Kauffman invariant to the Potts model shows that, if the variable x were not entering into an expression for the degeneracy of the energy level $H(E; q = 2+x+x^{-1})$, the maximum power of the polynomial invariant would always correspond to a term of the partition function with the minimum energy.

Taking into account dependence of the degree of degeneracy on the variable x, we can see that contributions to the coefficient at this power in some cases mutually cancel each other and this coefficient turns zero. A simple example is offered by a system free of impurities, in which case the minimum energy is $E_{min} = -(N+1)/2$ and the Jones polynomial is identically unity (with the maximum power being zero).

Nevertheless, there is a strong correlation between the maximum power n of the Jones polynomial and the minimum energy E_{min} of the corresponding Potts model. Since the minimum energy E_{min} of the Potts model is always sign-definite and cannot be positive, we use below a positive quantity representing the absolute value of the minimum energy $|E_{min}| = -E_{min}$. Figure 6a shows a joint probability distribution $P\left(\frac{n}{N}, \frac{|E_{min}|}{N}\right)$ of the normalized maximum power $\frac{n}{N}$ and the normalized minimum energy $\frac{|E_{min}|}{N}$ obtained for a lattice with $N = 49$ and an impurity concentration of $p = 0.5$ by averaging over $N_L = 10^5$ impurity configurations. Here and below we use only the normalized quantities determined on the $[0, 1]$ segment for the energy and $[-1, 1]$ for the maximum power of the polynomial (the latter value can be negative). This allows us to plot the curves for various lattice dimensions on the same figure. In Fig.6a, the probability distribution is described by the level curves, the spacing between which corresponds to a probability difference of 0.001. As can be seen, there is a strong correlation between the maximum power of the polynomial invariant and the

minimum energy of the corresponding Potts model. This relationship can be quantitatively characterized by the the coefficient of correlation.

It should be recalled that the coefficient of correlation between random quantities x_1 and x_1 with mathematical expectations $\langle x_1 \rangle$ and $\langle x_2 \rangle$ and dispersions $\Delta x_1 = \langle x_1^2 \rangle - \langle x_1 \rangle^2$ and $\Delta x_2 = \langle x_2^2 \rangle - \langle x_2 \rangle^2$, (where $\langle \ldots \rangle$ denotes averaging) is determined by the formula

$$\mathrm{corr}(x_1, x_2) = \frac{\langle x_1 x_2 \rangle - \langle x_1 \rangle \langle x_2 \rangle}{\sqrt{\Delta x_1 \Delta x_2}}$$

The correlation coefficient equal to ± 1 corresponds to a linear relationship between x_1 and x_2.

The values of the coefficient of correlation between the maximum power n_{max} of the polynomial invariant and the minimum energy $|E_{min}|$ for the impurity concentration $p = 0.5$ on lattices with various the linear dimensions $L = 3, 5, 7, 9$, and 11 are presented in Table 1. These values were obtained by averaging over $N_L = 10^5$ impurity realizations for $L = 3 \div 7$, $N_L = 2 \times 10^4$ for $L = 9$, and $N_L = 10^3$ for $L = 11$. As is seen, the correlation increases with the lattice size.

TABLE 1. Mean value of the correlation coefficient $\mathrm{corr}\,(n_{max}, |E_{min}|)$ and the corresponding statistical error for several lattice sizes.

L	$\mathrm{corr}\,(n, \lvert E_{min}\rvert)$	$\Delta\mathrm{corr}\,(n, \lvert E_{min}\rvert)$
3	0.4871	0.0021
5	0.6435	0.0022
7	0.7205	0.0007
9	0.7692	0.0013
11	0.7767	0.0129

Figure 6b shows the approximation of these data by a power function $\mathrm{corr}\left(\frac{n}{N}, \frac{|E_{min}|}{N}\right) = 1.04(4) - 1.126(14)L^{-0.65(7)}$. Naturally, the correlation coefficient cannot be greater than unity. The last expression is the result of ignoring the higher terms of expansion in powers of $\frac{1}{L}$. The approximation shows that there is a relationship between the maximum power of the polynomial invariant and the minimum energy of the Potts model, the degree of correlation increasing with the lattice size. In what follows, the results for the maximum power of the polynomial invariant will be accompanied by data for the minimum energy.

The presence of a correlation between the maximum power n of the Kauffman polynomial invariant and the minimum energy E_{min} of the corresponding Potts model for each particular impurity realization on the lattice is of interest from theoretical standpoint and can be used in the numerical experiments. At present, the limiting lattice size N_L used in the method of transfer matrix does not exceed $N_L = 11$, which is determined by a large volume of necessary computations. At the same time, the minimum energy for the Potts model can be calculated within the framework of the standard Monte-Carlo algorithm, which poses a much smaller requirements to the computational facilities and, hence, can be readily applied to the lattices of significantly greater size.

B. The probability distribution of the maximum power of the polynomial invariant and the minimum energy of the corresponding Potts model

Here we present the results of determining the probability distribution $P(n)$ of the maximum polynomial power n. Figure 7a shows the $P(n)$ curves for $L = 7$ and the impurity concentrations $p = 0.1$ (depicted by crosses), 0.2 (squares), and 0.5 (circles). The data were obtained by averaging over $N_L = 10^5$ impurity realizations. The statistical errors are smaller than the size of symbols.

As can be seen, the $P\left(\frac{n}{N}\right)$ curve for small impurity concentrations is nonmonotonic. As the p value increases, the probability distribution function becomes monotonic and approaches in shape to the Gauss function. Figure 7b shows the corresponding probability distribution of the normalized minimum energy $\frac{|E_{min}|}{N}$ obtained for the same lattice size ($L = 7$) and impurity concentrations (denoted by the same symbols). This function appears as more monotonic and approaches the Gauss function already at small impurity concentrations ($p \simeq 0.2$).

The shapes of the probability distribution observed for a fixed impurity concentration ($p = 0.5$) and various lattice dimensions are shown in 11a (for the maximum polynomial power) and Fig.11b (for the minimum energy). Data for the lattice size $L = 3$ (squares), 5(*squares*), and 7 (circles), and 9 (triangles) were averaged over $N_L = 10^5$ ($L = 3, 5$, and 7) and data for $L = 9$, over $N_L = 5 \times 10^3$ impurity realizations. The probability was normalized to unity: $\sum\limits_n P(n) = 1$ For this reason, an increase in the lattice size is accompanied by growing number of the values that can be adopted by the normalized maximum power of $P(\frac{n}{N})$, while the value of the probability distribution decreases approximately as $\frac{1}{N}$. As is seen, the probability distribution $P\left(\frac{n}{N}\right)$ for lattices of smaller size ($L = 3$ and 5) is nonmonotonic; as the L value increases, the distribution becomes a smooth Gaussian-like function.

Thus, we may conclude that the probability distribution $P\left(\frac{n}{N}\right)$ of the maximum power of the polynomial invariant for small-size lattices is nonmonotonic as a result of the boundary effects even for a considerable impurity concentration. As the lattice size increases, the nonmonotonic character disappears and the probability distribution becomes a smooth function. Apparently, we may ascertain that, whatever small is the impurity concentration p, there is a lattice size N ($N \gg \frac{1}{p}$) such that the corresponding probability distribution is smooth and Gaussian-like. Thus, we may suggest that the probability distribution $P(n)$ on the lattices of large size is determined by the Gauss function, the main parameters of which are the mathematical expectation (mean value) of the maximum polynomial power and the dispersion. Plots of the mean value of the maximum polynomial power $\left\langle \frac{n}{N} \right\rangle$ and the corresponding dispersion W^2_{knot} as functions of the impurity concentration p are presented in Figs. 9a and Fig.9, respectively, for the lattices size of $L = 3$ (crosses), 5 (squares), and 7 (circles). The data for each point were obtained by averaging over $N_L = 10^5$ impurity realizations for $L = 3$ and 5 and $N_L = 5 \times 10^4$ for $L = 7$.

As expected, both the mean value and the dispersion of the maximum polynomial power turn zero for $p = 0$ and 1 (trivial knot) and reach maximum at $p \simeq 0.5$. Note that these functions are not symmetric with respect to the transformation $p \to 1 - p$, since the Jones polynomial invariant of a mirror knot (with all overcrossing changed for undercrossing and vice versa) is obtained by changing variables $x \to x^{-1}$, whereby the maximum polynomial

power of the mirror knot corresponds to the minimum power of the original polynomial, taken with the minus sign. However, this asymmetry disappears with increasing lattice size N as a result of increase in the amount of impurities and in the number of possible impurity realizations employed in the averaging. For the comparison, Fig.9b shows the function $\frac{1}{2}p(1-p)$ representing the dispersion of the distribution function in the hypothetical case when the maximum polynomial power n is a linear function of the number of impurities M. Thus, a difference between W^2_{knot} and $\frac{1}{2}p(1-p)$ characterizes dispersion of the distribution of the maximum polynomial power at a fixed number of impurities M (it should be recalled that the impurity occupies each lattice site with a probability p and the total number of impurities M fluctuates).

Figures 10a and 10b (with the parameters and notations analogous to those in Fig.9a and Fig.9b) shows data for the absolute value of the mean minimum energy $\left\langle \frac{|E_{min}|}{N} \right\rangle$ and the corresponding dispersion W^2_{Potts}. The asymmetry of the mean minimum energy plot is related to the fact that the number of f-bonds is greater than that of the a-bonds by one at $p = 0$ and is smaller by one, at $p = 1$. The probability distribution of the minimum energy is treated in more detail in Subsection A 2 of the Appendix. We have studied dependence of the mean normalized maximum polynomial power on the lattice size L for $p = 0.5$ (Fig.11a). The results were averaged over $N_L = 10^5$ impurity realizations for $L = 3, 5$, and 7 and over $N_L = 1.5 \times 10^4$ realizations for $L = 9$. As can be seen, the $\left\langle \frac{n}{N} \right\rangle$ value tends to a certain limit with increasing $L \to \infty$. We approximated the results by a power function to obtain

$$\left\langle \frac{n}{N} \right\rangle \simeq 0.334(8) - 0.41(2)L^{-0.48(5)} \tag{21}$$

Analogous data for the normalized minimum energy in the Potts model are depicted in Fig.11b. The mean absolute value of the minimum energy decreases with increasing lattice size and can be approximated by a power function of the type

$$\left\langle \frac{|E_{min}|}{N} \right\rangle \simeq 0.4185(7) + 0.119(3)L^{-1.11(4)}$$

Some features of the minimum energy distribution in the Potts model with random ferro- and antiferromagnetic bonds are treated in the Appendix for $q \geq 4$, in which case analytical expressions can be obtained for small ($p \simeq 0$) and large ($p \simeq 1$) impurity concentrations.

V. CONCLUSIONS

The results of this investigation can be formulated as follows.

1. An analysis of the relationship between the partition function of the Potts model and the Jones-Kauffman polynomial invariant, in combination with the results of numerical calculations for the Potts model, allowed us to study the probability distribution $P(\frac{n}{N}; p, N)$ of the maximum polynomial power n for various concentrations (probabilities) p of an "impurity" representing intersections of the $\epsilon = -1$ type in the sites of a square lattice with $N = L \times L$ for $L = 3 - 11$.

2. For the lattices of small size with small impurity concentrations p, the probability distribution $P(\frac{n}{N}; p, N)$ of the normalized maximum polynomial invariant power n is not

smooth, showing an alternation of more and less probable states. This behavior indicates that the knots of certain topological types are difficult to realize for $p \ll 1$ on a square lattice as a result of geometric limitations.

3. As the impurity concentration (probability) p increases, the probability distribution $P(\frac{n}{N}; p, N)$ of the normalized maximum polynomial invariant power n becomes smooth, with the shape approaching that of the Gauss function. A typical value of the "knot complexity" η for $p = 0.5$ and sufficiently large lattices ($N \gg 1$) can be obtained by extrapolating the expression (21):

$$\eta = \lim_{N\to\infty} \left\langle \frac{n}{N} \right\rangle \approx 0.334$$

4. There is a correlation between the maximum power of the polynomial invariant of a knot and the minimum energy of the corresponding Potts lattice model for $q \geq 4$.

5. An analytical expression was obtained for the probability distribution function $P(\frac{E_{min}}{N}; p, N)$ at relatively small $p \sim \frac{1}{N}$ impurity concentrations.

We have studied the knots with a square lattice diagram. However, all calculations can be generalized to the case of rectangular lattices. In connection with this, it would be of interest to check whether the distribution of knots over the topological types only depends on the number of intersections on the lattice diagram or it depends on the diagram shape as well. We may expect that the probability distribution function for a strongly elongated rectangular diagram would differ from the distribution for a square diagram with the same number of intersections.

The method developed in this study is applicable, in principle, to the investigation of knots with arbitrary diagrams (including the case of knots with the diagrams not tightly fit to a rectangular lattice), provided that a configuration of the Potts system corresponding to this diagram is known.

We believe that the proposed combination of analytical and numerical methods for the investigation of topological problems using the models of statistical physics offers both a promising means of solving such topological problems and a new approach to the standard methods of investigation of disordered systems. This can be illustrated by the following fact. One of the main concepts in the statistical physics is the principle of additivity of the free energy of a system, that is, proportionality of the free energy to the system volume N. By interpreting the free energy as a topological characteristic of the "complexity" of a knot, we may conclude that the complexity of a typical knot increases linearly with the system volume N. This property is, in turn, well known in the topology (outside the context of statistical physics), being a fundamental manifestation of the non-Abelian (non-commutative) character of the phase space of knots.

Acknowledgments

This study is a logical development of the ideas formulated by one of the authors in collaboration with A.Yu. Grosberg in 1992-1993 [12]. The authors are grateful to A.Yu. Grosberg for fruitful comments and to J.L. Jacobsen for helpful discussions concerning transfer–matrix approach. The study was partly supported by the russian Foundation for Basic Research, project no. 00-125-99302. One of the authors (O.A.V.) is grateful to the L.D. Landau Grant Committee (Forschungzentrum, KFA Julich, Germany) for support.

APPENDIX: MINIMUM ENERGY DISTRIBUTION IN THE POTTS MODEL WITH RANDOM FERRO- AND ANTIFERROMAGNETIC BONDS

1. Independence of the minimal energy upon q for $q \geq 4$

The minimum energy of a spin system is independent of q for $q \geq 4$. In this study of the topological invariants of random lattice knots, we are interested in determining behavior of the system for $x \to \infty$(see Eq. (20)). With an allowance for the relationship $q = 2 + x + x^{-1}$, this implies $q \to \infty$ for the corresponding Potts model. Some features of the dependence of the free energy of the Potts spin system on the number of states q can be established based on simple considerations. In cases when the lattice contains no impurities and the a-bonds are arranged as depicted in Figs.3b and 3c, the minimum energy is independent of q for $q \geq 2$. Under these conditions, two spin values $\sigma = \{1, 2\}$ are sufficient to "create" a configuration corresponding to the minimum energy. In the presence of impurities, the minimum energy depends on q for $q \geq 2$. This is illustrated in Fig.5a for a 5×5 lattice with a single impurity on the bond between $\sigma_{1,1}$ and $\sigma_{1,2}$ spins. For the spin configuration energy to reach a minimum value of $E_{min} = -12$ for the given distribution of bonds, it is necessary that all spin variables in the lattice sites connected by f-bonds $J = 1$ (in Fig.5, these sites are indicated by open and filled circles) would acquire the same values, while the spin variables in the sites $\sigma_{1,1}$ and $\sigma_{1,2}$ connected by a-bonds $J = -1$ (in Fig.5a, these sites are indicated by filled and hatched circles) would acquire different values (e.g., $\sigma_{1,1} = 2,\ \sigma_{1,2} = 3$). However, it is impossible to assign the values of spin variables in a system with $q = 2$ so that the spins in clusters $\sigma_{1,1},\ \sigma_{1,2}$ (as well as in the adjacent cluster) indicated by unlike symbols (black versus open or hatched) were different. For this reason, a minimum energy of the spin state for $q = 2$ is $E_{min} = -11$ (instead of -12).

As was demonstrated, a minimum energy of the spin configuration in the Potts model corresponding to a given distribution of a-bonds may depend on the number of spin states q. This fact can be represented as follows: to reach the state with minimum energy, it is necessary that the spin variables in the lattice sites connected by f-bonds would acquire for the most part the same values (so as to form clusters), while the spin variables in the sites connected by a-bonds would be possibly different. Thus, a given distribution of the a-bonds corresponds to a subdivision of the lattice into independent clusters of spins. Spins belonging to the same cluster are connected predominantly by the f-bonds, while spins of different clusters are connected by a-bonds.

The energy reaches minimum if the adjacent clusters in a given subdivision possess different values of the spin variable. We may bring each value of the spin variable into correspondence with a certain color. Then a minimum energy corresponds to the lattice subdivision into clusters painted so that all spins in one cluster are of the same color, whereas adjacent clusters have different colors. Figure 5a shows an example of the configuration which cannot be painted in this way using two colors, while three colors allow reaching the goal. In mathematics, there is a theorem concerning the task of "painting maps", according to which any configuration on a surface possessing a a topology of a sphere can be painted using four (or more) colors. In other words, any subdivision of a lattice into clusters can be painted using four (or more) colors so that the adjacent clusters would possess different colors. If each color corresponds to a certain value of the spin variable $q = \{1, 2, 3, 4, ...\}$,

we may assign the q values (for $q \geq 4$) so that spins in the adjacent clusters would possess different values (colors). There is no impurity configuration (and the corresponding lattice subdivision into clusters) such that four values of the spin variable would be insufficient to reach the state of minimum energy.

The above considerations allow us to formulate the following statement: For an arbitrary configuration of a-impurities on a Potts model lattice, a minimum energy of the spin system is independent of the number of spin states q for $q \geq 4$.

As is known, the Potts model exhibits a first-order phase transition at $q \geq 4$. Note also that the parameter in the Kauffman invariant becomes real just for $q \geq 4$.

2. Distribution of the minimum energy at small ($p \simeq 0$) and large ($p \simeq 1$) impurity concentrations

Consider the Potts model on an $L_v \times L_h$ lattice with a total number of lattice sites N and $q \geq 4$. Let M be a fixed number of impurities of the ϵ_k types. In the absence of impurities ($M = 0$), the number of f-bonds is $N_+ = \frac{N+1}{2}$ and the number of a-bonds is $N_- = \frac{N-1}{2}$. The arrangement of a-bonds is illustrated in Fig.5a. The minimum energy in the absence of impurities is $E_{min} = -N_+$.

TABLE 2. The probability distribution of energy $P(E_{min}; M, N)$ for a fixed number of impurities $M = 0, 1, 2, N-2, N-1, N$ on a lattice with Nsites ($C = \sqrt{N}$).

I	II	III	IV
M	Link type	E_{min}	$P(E_{min}; M)$
0		$-\frac{N+1}{2}$	1
1	+	$-\frac{N+1}{2}+1$	$\frac{N+1}{2N}$
1	−	$-\frac{N+1}{2}$	$\frac{N-1}{2N}$
2	++	$-\frac{N+1}{2}+2$	$\frac{(N+1)(N-1)}{4N(N-1)}$
2	+−	$-\frac{N+1}{2}+1$	$\frac{(N+1)(N-1)-16(C-1)}{2N(N-1)}$
2	+−&−−	$-\frac{N+1}{2}$	$\frac{(N-1)(N-3)+16(C-1)}{4N(N-1)}$
2	−−	$-\frac{N+1}{2}-1$	$\frac{4(C-2)}{N(N-1)}$
2	−−	$-\frac{N+1}{2}-2$	$\frac{4}{N(N-1)}$
N-2	++	$-\frac{N-1}{2}+2$	$\frac{(N-1)(N-3)}{4N(N-1)}$
N-2	+−	$-\frac{N-1}{2}+1$	$\frac{(N-1)(N-3)-16(C-1)}{2N(N-1)}$
N-2	+−&−−	$-\frac{N-1}{2}$	$\frac{(N+1)(N-1)+16(C-1)-4}{4N(N-1)}$
N-2	+−&−−	$-\frac{N-1}{2}-1$	$\frac{2(N-1)+2(C-1))}{N(N-1)}$
N-2	−−	$-\frac{N-1}{2}-2$	$\frac{2}{N(N-1)}$
N-1	+	$-\frac{N-1}{2}+1$	$\frac{N-1}{2N}$
N-1	−	$-\frac{N-1}{2}$	$\frac{N-3}{2N}$
N-1	−	$-\frac{N-1}{2}-1$	$\frac{2}{N}$
N		$-\frac{N-1}{2}$	1

We may calculate the probability distribution $P(E_{min}; M, N)$ of the minimum energy for $M = 1$ and 2 by trials of the possible variants. In the case of a single impurity ($M = 1$),

there is a probability $N_+/N = (N+1)/2N$ for this impurity to fall on the f-bond, after which the minimum energy increases by unity: $P(E = -N_+ + 1) = (N+1)/2N$ There is also the probability $N_-/N = (N-1)/2N$ for the impurity to fall on the a-bond, after which the minimum energy remains unchanged: $P(E = -(N+1)/2) = (N-1)/N$ Similar considerations can be conducted for $M = 2$. Let $C = \sqrt{N}$ denote the number of spin clusters with the same q on a lattice without impurities. The results of this analysis are summarized in Table 2, where each line indicates (I) the number of impurities M, (II) the coupling constant of a bond on which the impurity falls (with the signs "+" and "−" corresponding to $b_{i,j} = 1$and -1, respectively), (III) the minimum energy E_{min} and (IV) the probability $P(E_{min}; M)$ of obtaining a given minimum energy value.

With p denoting the probability that a bond contains the impurity $J' = -1$, the probability to find M impurities is $P(M; p) = \frac{N!}{M!(N-M)!}p^M(1-p)^{N-M}$. Thus, a mean value of the minimum energy E in the Potts model is

$$\langle E_{min}\rangle = \sum_{M=0}^{N} \frac{N!}{M!(N-M)!}p^M(1-p)^{N-M}P(E; M, N) \tag{A1}$$

Calculating the first three terms for this sum using the data in Table 2, we obtain an approximate formula for the mean minimum energy

$$\begin{aligned}\langle E_{min}\rangle \simeq (1-p)^{N-2}\ \Big((1-p)^2P(E; M=0) + Np(1-p)P(E; M=1) + \\ p^2P(E; M=2)\Big) + o(p^2)\end{aligned} \tag{A2}$$

This formula is applicable if the probability for three impurities to appear on the lattice is small, that is, if $\frac{1}{6}N(N-1)(N-2)(1-p)^{N-3}p^3 \ll 1$ Upon calculating the probability of the impurity concentration for $M = 1$ and 2 and using expression (A1), we obtain a formula for $\langle E_{min}\rangle$ at small p. For example, in the case of $M = 1$ this yields

$$\langle E_{min}(M=1)\rangle = \left(-\frac{N+1}{2}\right)\left(\frac{N-1}{2N}\right) + \left(-\frac{N+1}{2}+1\right)\left(\frac{N+1}{2N}\right) = -\frac{N+1}{2} + \frac{N+1}{2N}$$

By the same token, for $M = 2$ we obtain

$$\langle E_{min}(M=2)\rangle = -\frac{N+1}{2} + \frac{N+1}{N} - \frac{12C-8}{N(N-1)}$$

Using these expressions and taking into account that $C = \sqrt{N}$, we obtain an expression for the mean normalized minimum energy $< e_{min} >= \left\langle \frac{E_{min}}{N} \right\rangle$ as a function of the impurity concentration p (in the case of $p \ll 1$)

$$\begin{aligned}< e_{min}(p) > \ = \ \tfrac{1}{N}\Big[(1-p)^N P(E; M=0) + Np(1-p)^{N-1}P(E; M=1) + \\ \frac{1}{2}N(N-1)p^2(1-p)^{N-2}P(n; M=2) + o(p^2)\Big] = \\ -\frac{1}{2}\left(1-\frac{1}{N}\right) + p\frac{1}{2}\left(1-\frac{3}{N}\right) - p^2\frac{6\sqrt{N}-4}{N} + o(p^2)\end{aligned} \tag{A3}$$

Analogous calculations for the concentrations $1-p \ll 1$ yield

$$\langle E_{min}(M=N-1)\rangle = -\frac{N-1}{2} + \frac{N-5}{2N}$$
$$\langle E_{min}(M=N-2)\rangle = -\frac{N-1}{2} + \frac{N-5}{N} - \frac{10C-14}{N(N-1)}$$

and

$$< e_{min}(p) > = \frac{1}{N}\Big[p^N P(E;M=N) + N(1-p)p^{N-1}P(E;M=N-1) + \frac{1}{2}N(N-1)(1-p)^2 p^{N-2}P(n;M=N-2) + o(p^2)\Big] = -\frac{1}{2}\left(1-\frac{1}{N}\right) + (1-p)\frac{1}{2}\left(1-\frac{5}{N}\right) - (1-p)^2\frac{5\sqrt{N}-7}{N} + o((1-p)^2) \quad \text{(A4)}$$

The results of calculations using the formulas presented in Table 2 and the results of numerical analysis for $q=4$, $L_v=3$, and $L_h=6$ (corresponding to a knot with a $5times5$ square lattice diagram) are plotted in Fig.12a in coordinates of the minimum energy modulus versus probability. Figure 12a shows the results for a fixed number of impurities $M=1$ (squares) and 2 (circles), while Fig.12b presents data for the fixed impurity con-centrations $p=0.005$ (crosses), 0.01 (squares), and 0.015 (circles). The results of calculations using the formulas from Table 2 and relationship (A2) are depicted by lines and the values obtained by the Monte Carlo method are represented by symbols. The data were averaged over $N_L=10^5$ realizations; the statistical error for most of the points is smaller than the size of symbols. As can be seen, the numerical data remarkably fit to the analytical curves. In 12b, the analytical calculations are illustrated only in the range $|E_{min}|=11\div15$, where the results could be obtained by expansion into series with terms on the order of p^2 . Thus, we have numerically verified the results of analytical calculations performed in this section.

Let us make some remarks concerning the form of the normalized minimum energy $< e_{min}(p;N) >= \left\langle \frac{|E_{min}(p;N)|}{N} \right\rangle$ for $N \to \infty$. As can be seen in Fig.9b, the plots of $< e_{min}(p;N) >= \left\langle \frac{|E_{min}(p;N)|}{N} \right\rangle$ for the lattices with $N=25$ and 49 appear as asymmetric troughs. As $N \to \infty$, the values of this function at $p=0$ and 1

$$< e_{min}(p=0;N) >= 0.5\left(1+\frac{1}{N}\right)$$

and

$$< e_{min}(p=1;N) >= 0.5\left(1-\frac{1}{N}\right)$$

will be equal and the profiles will be symmetric with respect to the transformation $p \to 1-p$. The bottom will occur on a level of $< e(p=0.5;N\to\infty) >= 0.415(7)$ (see Fig.11b). As can be seen from formulas (A3) and (A4), the second derivative of this function with respect to p at the points $p=0$ and 1 turns zero for $N \to$. Probably, all derivatives of the higher orders will turn zero as well. In this case, the derivative exhibits a break at the points corre-sponding to the trough "corners."

[1] S.K. Nechaev, Usp.Fiz.Nauk **168**, 369 (1998) [Sov.Phys. Uspekhi, **41**, 313 (1998)].
[2] M.D. Frank-Kamenetskii and A.V. Vologodskii, Usp. Fiz. Nauk **134**, 641 (1981) [Sov.Phys. Uspekhi **24**, 679 (1981)]; A. V. Vologodskii et al., Zh.Eksp.Teor.Fiz. **66**, 2153 (1974) [Sov.Phys. JETP **39**, 1059 (1974)]; A.V. Vologodskii, A.V. Lukashin, and M.D. Frank-Kamenetskii, Zh.Eksp.Teor.Fiz. **67**, 1875 (1974) [Sov.Phys. JETP **40**, 932 (1975)]; M.D. Frank-Kamenetskii, A.V. Lukashin, and A.V. Vologodskii, Nature (London) **258**, 398 (1975).
[3] V.F.R. Jones, Ann.Math., **126**, 335 (1987)
[4] V.F.R. Jones, Bull.Am.Math.Soc. **12**, 103 (1985)
[5] J. Birman, *Knots, Links and Mapping Class Groups*, Ann.Math.Studies, **82** (Princeton Univ. Press, 1976)
[6] A.B. Sosinskii and V.V. Prasolov, *Knots, Links, Braids and Three-dimensional Manifolds* (Nauka, Moscow, 1998).
[7] R.J. Baxter, *Exactly Solved Models in Statistical Mechanics* (Academic, New York, 1982; Mir, Moscow, 1985).
[8] W.B.R. Likorish, Bull.London Math.Soc., **20**, 558 (1988); M. Wadati, T.K. Deguchi, Y. Akutso, Phys.Rep., **180**, 247 (1989)
[9] L.H. Kauffman, Topology, **26**, 395 (1987)
[10] L.H. Kauffman, H. Saleur, Comm. Math. Phys., **141**, 293 (1991)
[11] F.Y. Wu, J. Knot Theory Ramific., **1** 47 (1992)
[12] A.Yu. Grosberg, S. Nechaev, J. Phys. (A): Math. Gen., **25**, 4659 (1992); A.Yu. Grosberg, S. Nechaev, Europhys.Lett., **20**, 613 (1992)
[13] H.W. Blote and M.P. Nightingale, Physica A, **112**, 405 (1982)
[14] J.L. Jacobsen and J. Cardy, cond-mat/9711279; Nucl.Phys. B, **515** [FS], 701 (1998)
[15] J. Salas and A.D. Sokal, cond-mat/0004330; J.Stat.Phys., **104**, 609 (2001)
[16] A.Yu. Grosberg, S.K. Nechaev, E.I. Shakhnovich, J.Phys. (Paris), **49**, 2095 (1988)
[17] B. Chu, Q. Ying, A. Grosberg, Macromolecules, **28** (1995), 180; A. Grosberg, Y. Rabin, S. Havlin, A. Neer, Europhys.Lett., **23**, 373 (1993); J. Ma, J.E. Straub, E.I. Shakhnovich, J. Chem. Phys., **103**, 2615 (1995)
[18] K. Reidemeister, *Knotentheorie* (Berlin: Springer, 1932)
[19] F.Y. Wu, Rev.Mod.Phys. **54**, 235 (1982)
[20] C.M. Fortuin and P.M. Kastelleyn, Physica **57**, 536 (1972)
[21] R.H. Swedsen and J.S. Wang, Phys.Rev.Lett., **58**, 86 (1987)
[22] U. Wolff, Phys.Rev.Lett., **62**, 361 (1988)

Figure Captions

Fig.1. **a)** A knot diagram on the $N = 3 \times 3$ lattice and **b)** the diagram splitting. Open circles indicate the spin positions in the Potts model; dashed lines show the graphs on the Potts lattice.

Fig.2. The Reidemeister moves I, II, and II.

Fig.3. **a)** A knot on $N = 5 \times 5$ lattice; **b)** Potts spin configuration corresponding to this lattice, and **c)** the same spin configuration reduced to a rectangular lattice $L_h \times L_v = 3 \times 6$.

Fig.4. A schematic diagram illustrating the step-by-step generation of subdivisions into clusters for a column of spins corresponding to the knot state vectors.

Fig.5. **a)** An example of the configuration of bonds in which a minimum energy of the Potts model is not reached for $q = 2$; **b), c)** the arrangement of f- and a-bonds on the Potts lattice with $N = 3 \times 3$ and the impurity concentrations $p = 0$ and $p = 1$, respectively; (c, d) the arrangement of bonds between col- umns with even and odd numbers, respectively.

Fig.6. **a)** A joint probability distribution $P\left(\frac{n}{N}, \frac{E_{min}}{N}\right)$ of the normalized maximum polynomial power $\frac{n}{N}$ and the normalized minimum energy $\frac{E_{min}}{N}$ described by the level curves with a step of 0.001 for a lattice with $N = 49$ and an impurity concentration of $p = 0.5$; **b)** The coefficient of correlation between the maximum power of the polynomial invariant and the minimum energy as a function of the lattice size L; dashed curve shows the approximation of these data by a power function of L.

Fig.7. The distributions of **a)** probability $P(\frac{n}{N}; p)$ of the normalized maximum polynomial power $\frac{n}{N}$ and **b)** probability $P\left(\frac{|E_{min}|}{N}; p\right)$ of the normalized minimum energy modulus E_{min} for a 7×7 lattice and various impurity concentrations $p = 0.1, 0.2$ and 0.5.

Fig.8. The probability of **a)** the normalized maximum polynomial power $\frac{n}{N}$ and **b)** the normalized minimum energy modulus $\frac{|E_{min}|}{N}$ for the square lattices with $N = 9, 25, 49$, and 81 and an impurity concentration of $p = 0.5$.

Fig.9. Plots of **a)** the mean normalized maximum polynomial power $\left\langle \frac{n}{N} \right\rangle$ and **b)** the dispersion $W^2_{knot}(p)$ of the $\frac{n}{N}$ value distribution versus the impurity concentration p in the range from 0 to 10.

Fig.10. Plots of **a)** the mean normalized minimum energy modulus $\left\langle \frac{|E_{min}|}{N} \right\rangle$ and **b)** the dispersion $W^2_{Potts}(p)$ of the $\frac{|E_{min}|}{N}$ value distribution versus the impurity concentration p in the range from 0 to 10.

Fig.11. Plots of **a)** the mean normalized maximum power $\left\langle \frac{n}{N} \right\rangle$ of the polynomial invariant and **b)** the normalized mean minimum energy modulus $\left\langle \frac{|E_{min}|}{N} \right\rangle$ for the square lattices with $L = \sqrt{N} = 3, 5, 7$, and 9 and an impurity concentration of $p = 0.5$; dashed curve in **b)** shows the results of approximation by the power function $0.4185(7) + 0.119(3)L^{-1.11(4)}$.

Fig.12. A comparison of the results obtained by analytical (anal.) and numerical (num.) methods for the minimum energy probability distributions on a lattice with $N = 5 \times 5$: **a)** $P(|E_{min}|; M)$ with $M = 1$ and 2; **b)** $P(|E_{min}|; p)$ with $p = 0.005, 0.01$, and 0.015.

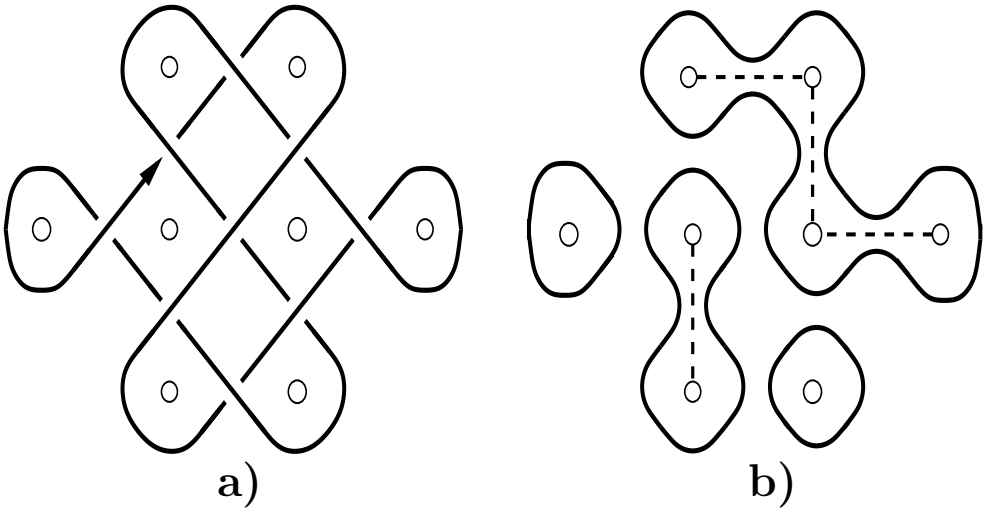

FIG. 1.

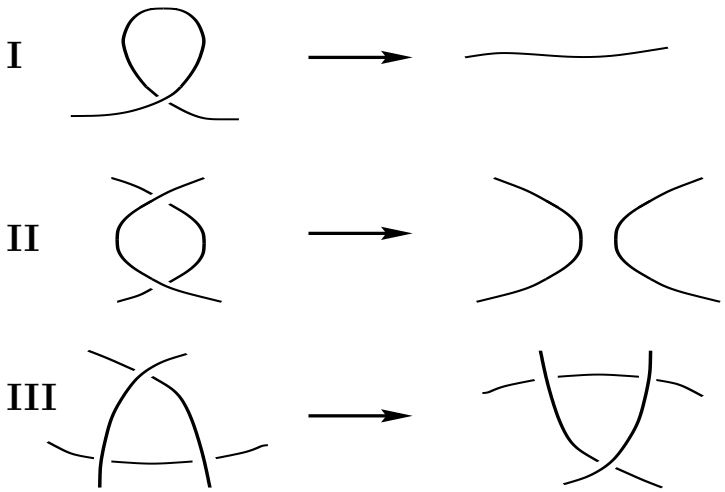

FIG. 2.

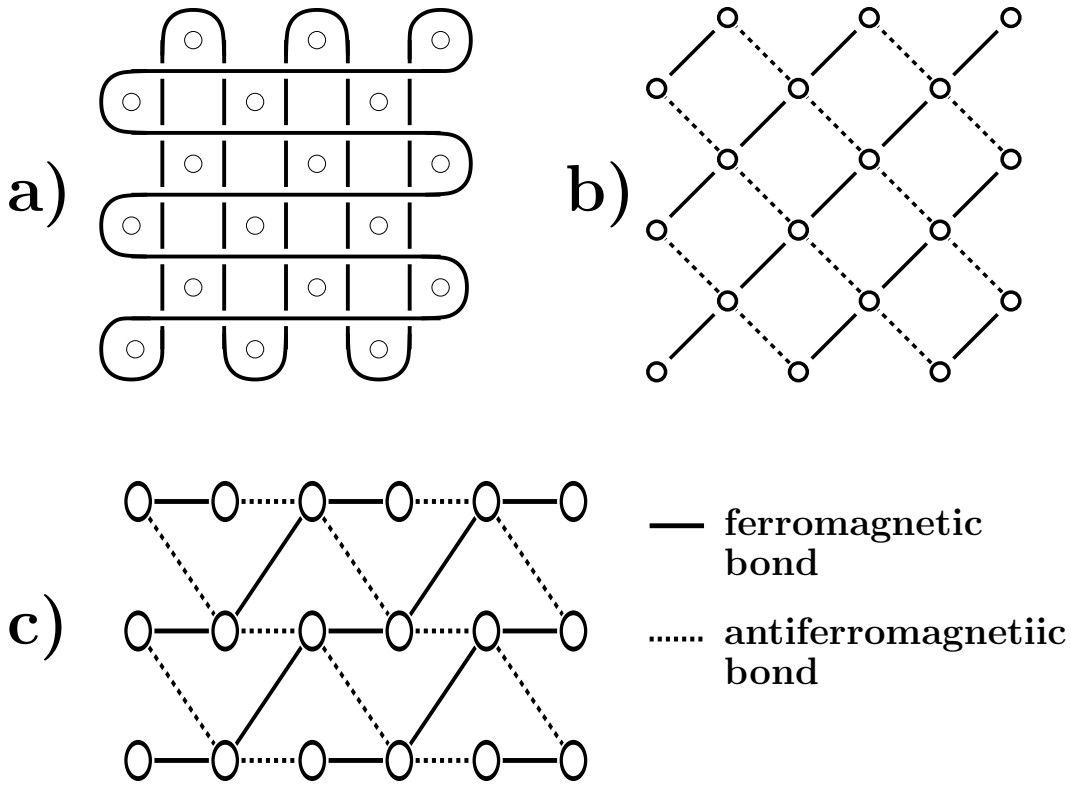

FIG. 3.

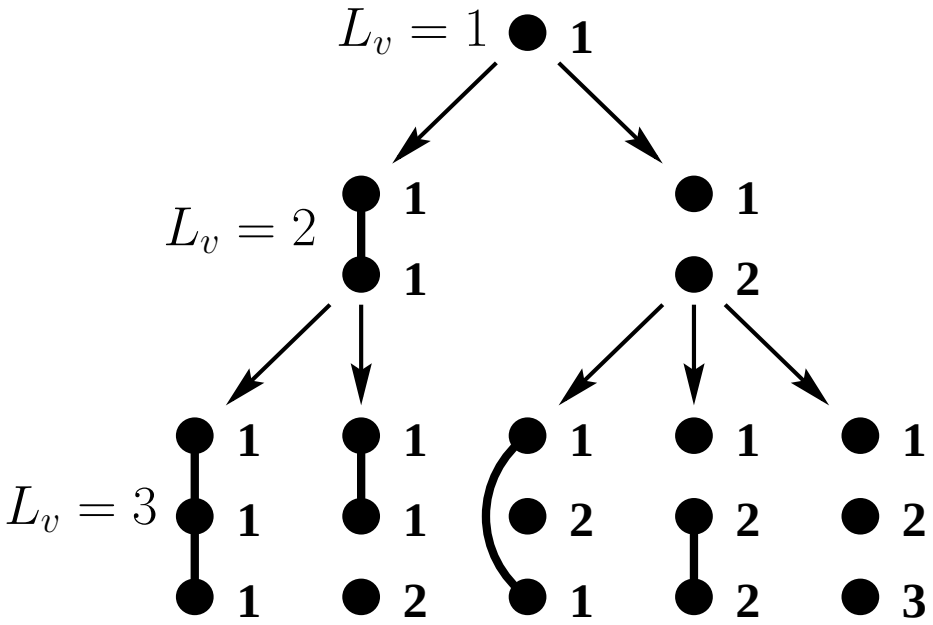

FIG. 4.

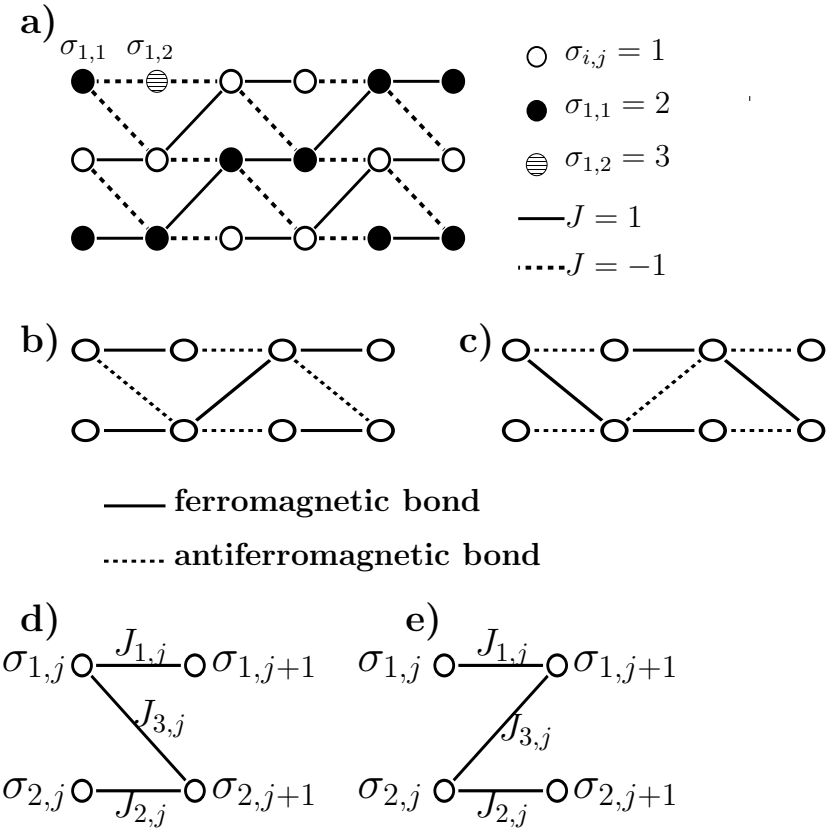
a)
$\sigma_{1,1}$ $\sigma_{1,2}$
$\sigma_{i,j} = 1$
$\sigma_{1,1} = 2$
$\sigma_{1,2} = 3$
$J = 1$
$J = -1$
b)
c)
ferromagnetic bond
antiferromagnetic bond
d)
$\sigma_{1,j}$ $J_{1,j}$ $\sigma_{1,j+1}$
$J_{3,j}$
$\sigma_{2,j}$ $J_{2,j}$ $\sigma_{2,j+1}$
e)
$\sigma_{1,j}$ $J_{1,j}$ $\sigma_{1,j+1}$
$J_{3,j}$
$\sigma_{2,j}$ $J_{2,j}$ $\sigma_{2,j+1}$

FIG. 5.

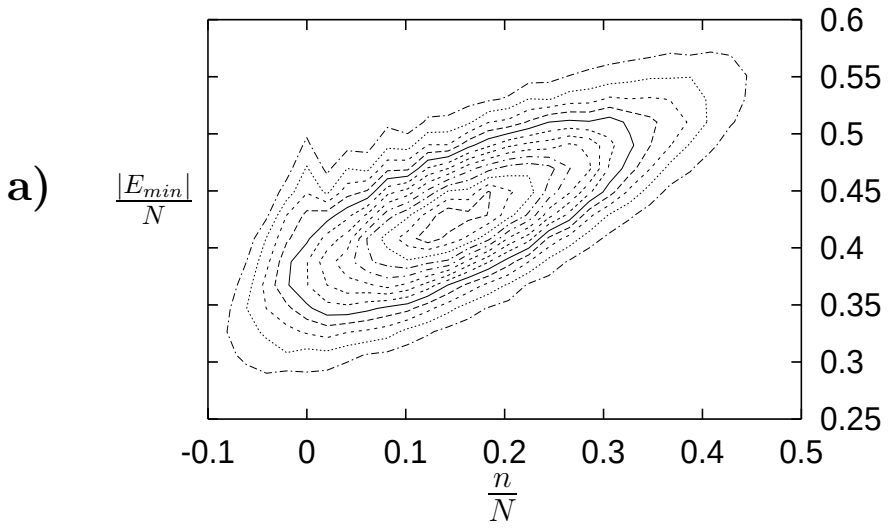
a)
$\frac{|E_{min}|}{N}$
0.6
0.55
0.5
0.45
0.4
0.35
0.3
0.25
-0.1
0
0.1
0.2
0.3
0.4
0.5
$\frac{n}{N}$

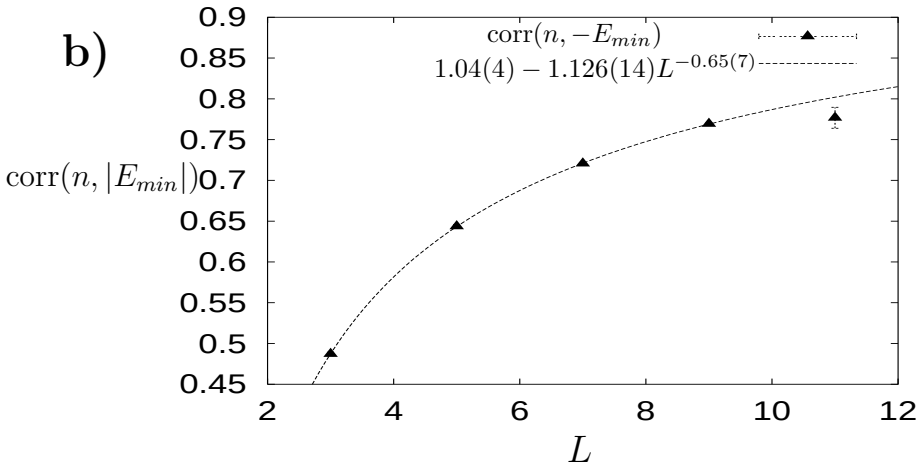
b)
$\mathrm{corr}(n, |E_{min}|)$
$\mathrm{corr}(n, -E_{min})$
$1.04(4) - 1.126(14)L^{-0.65(7)}$
0.9
0.85
0.8
0.75
0.7
0.65
0.6
0.55
0.5
0.45
2
4
6
8
10
12
L

FIG. 6.

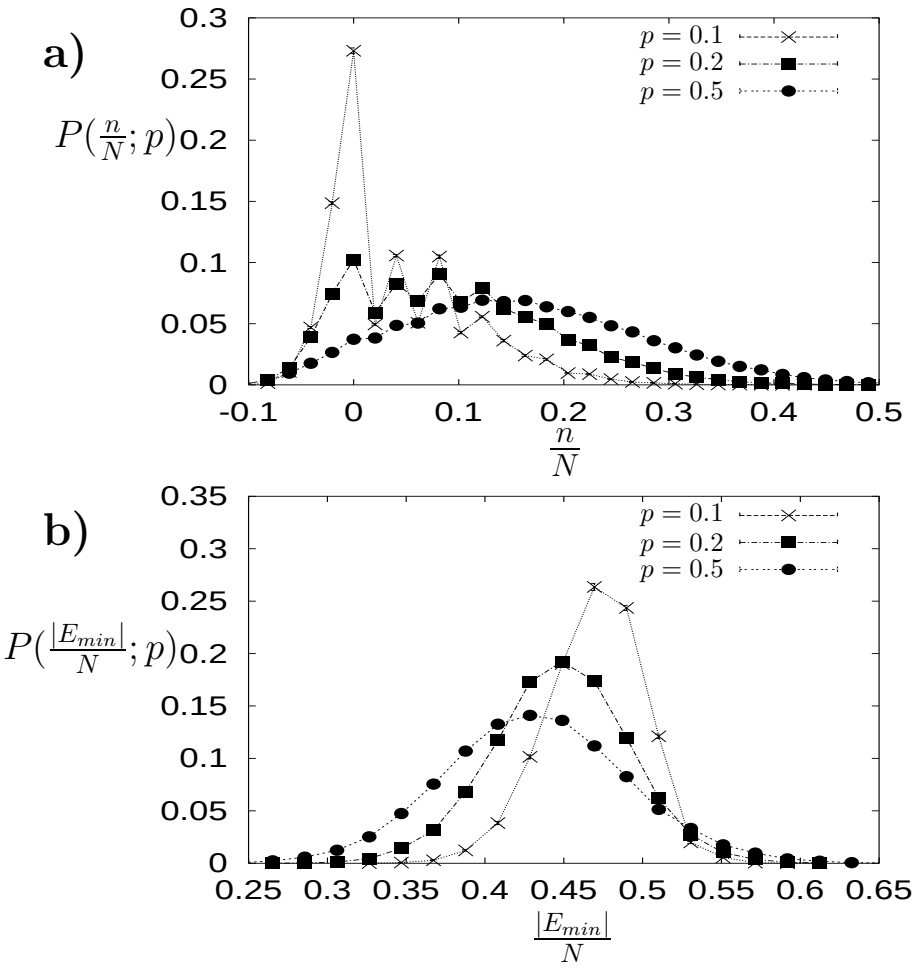
a)
$P(\frac{n}{N};p)$
$p = 0.1$
$p = 0.2$
$p = 0.5$
$\frac{n}{N}$
b)
$P(\frac{|E_{min}|}{N};p)$
$p = 0.1$
$p = 0.2$
$p = 0.5$
$\frac{|E_{min}|}{N}$

FIG. 7.

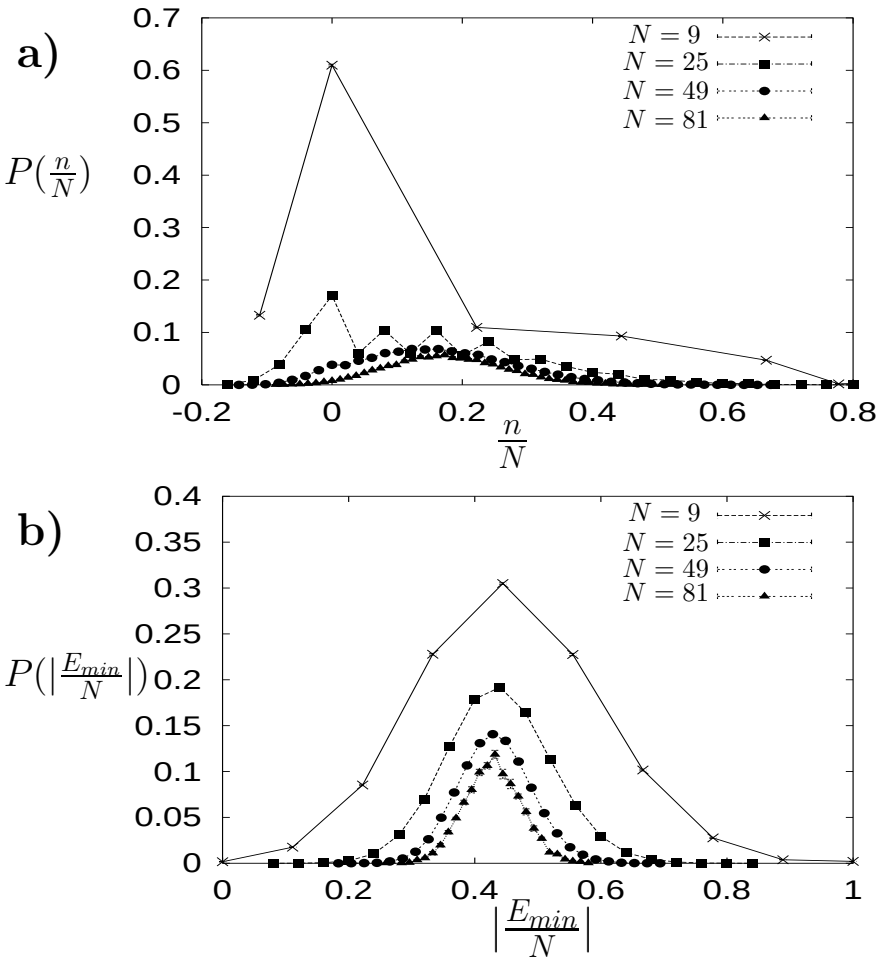
a)
$P(\frac{n}{N})$
$N = 9$
$N = 25$
$N = 49$
$N = 81$
0.7
0.6
0.5
0.4
0.3
0.2
0.1
0
-0.2
0
0.2
0.4
0.6
0.8
$\frac{n}{N}$
b)
$P(|\frac{E_{min}}{N}|)$
$N = 9$
$N = 25$
$N = 49$
$N = 81$
0.4
0.35
0.3
0.25
0.2
0.15
0.1
0.05
0
0
0.2
0.4
0.6
0.8
1
$|\frac{E_{min}}{N}|$

FIG. 8.

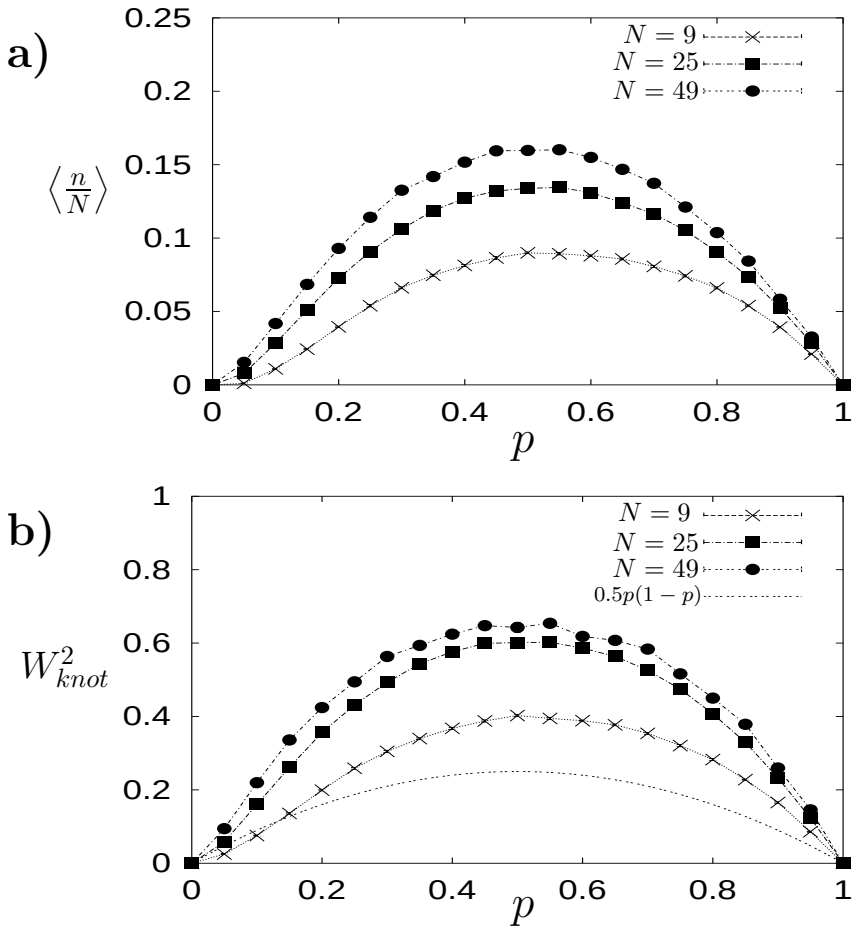
a)
0.25
0.2
0.15
0.1
0.05
0
$\left\langle \frac{n}{N} \right\rangle$
$N = 9$
$N = 25$
$N = 49$
0
0.2
0.4
0.6
0.8
1
p
b)
1
0.8
0.6
0.4
0.2
0
W^2_{knot}
$N = 9$
$N = 25$
$N = 49$
$0.5p(1-p)$
0
0.2
0.4
0.6
0.8
1
p

FIG. 9.

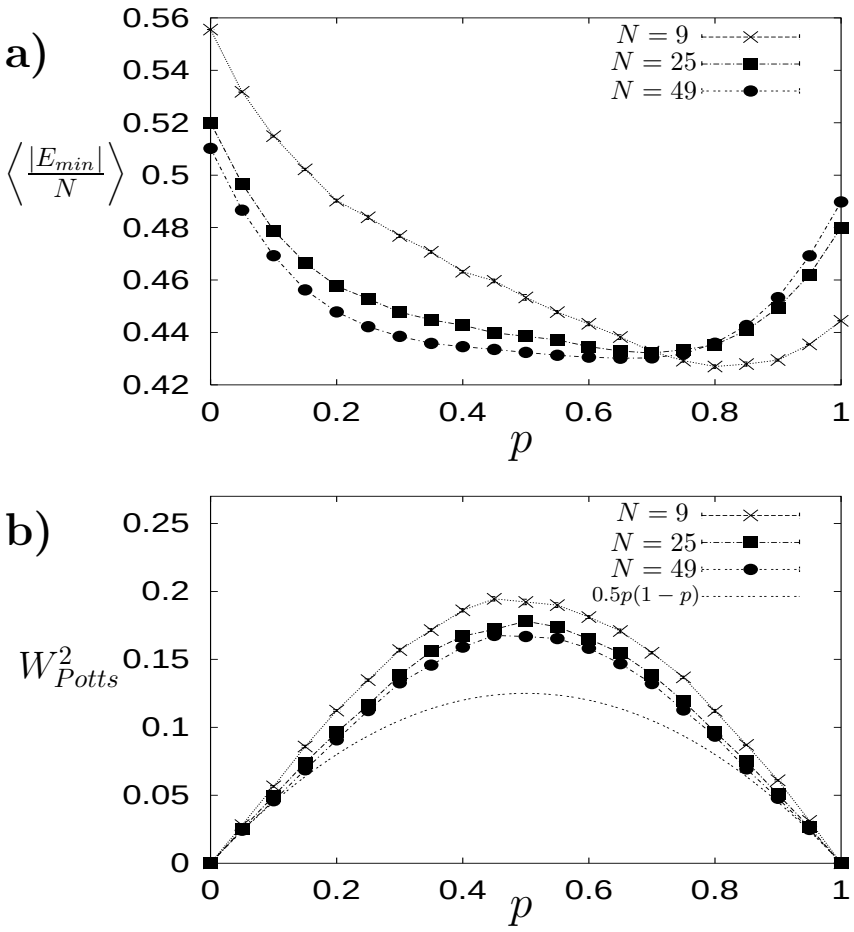
a)
$\left\langle \frac{|E_{min}|}{N} \right\rangle$
0.56
0.54
0.52
0.5
0.48
0.46
0.44
0.42
0
0.2
0.4
0.6
0.8
1
p
$N = 9$
$N = 25$
$N = 49$
b)
W^2_{Potts}
0.25
0.2
0.15
0.1
0.05
0
0
0.2
0.4
0.6
0.8
1
p
$N = 9$
$N = 25$
$N = 49$
$0.5p(1-p)$

FIG. 10.

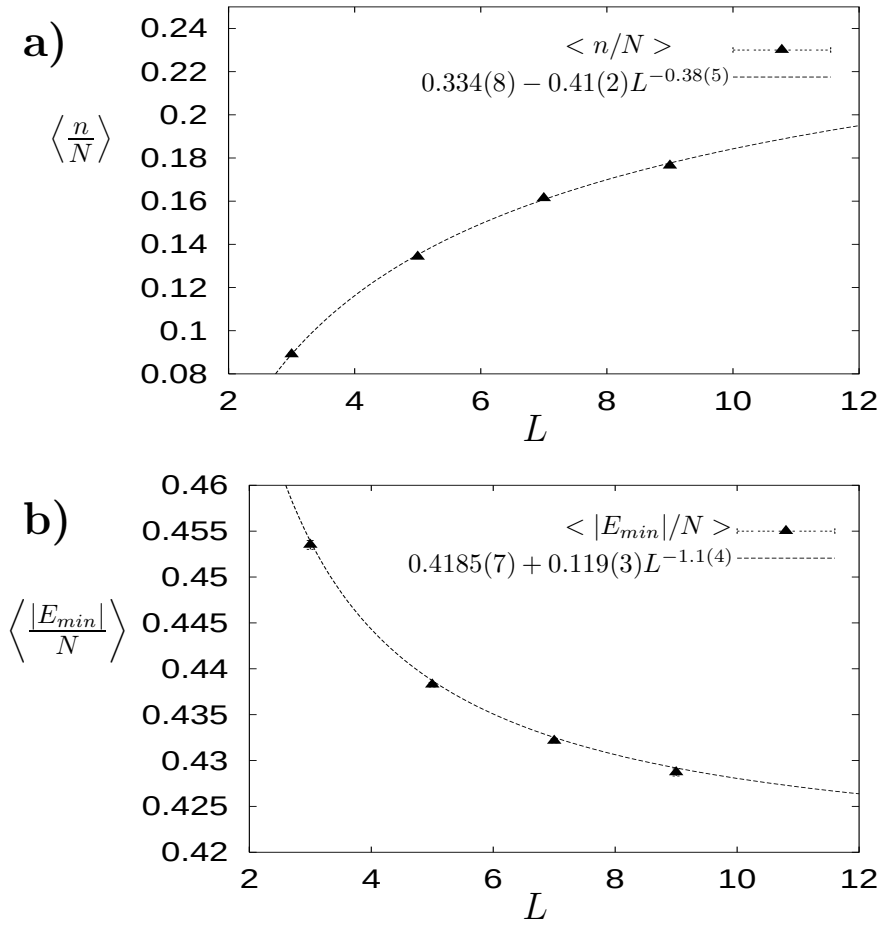
a)
$\left\langle \frac{n}{N} \right\rangle$
$< n/N >$
$0.334(8) - 0.41(2)L^{-0.38(5)}$
0.24
0.22
0.2
0.18
0.16
0.14
0.12
0.1
0.08
2
4
6
8
10
12
L
b)
$\left\langle \frac{|E_{min}|}{N} \right\rangle$
$< |E_{min}|/N >$
$0.4185(7) + 0.119(3)L^{-1.1(4)}$
0.46
0.455
0.45
0.445
0.44
0.435
0.43
0.425
0.42
2
4
6
8
10
12
L

FIG. 11.

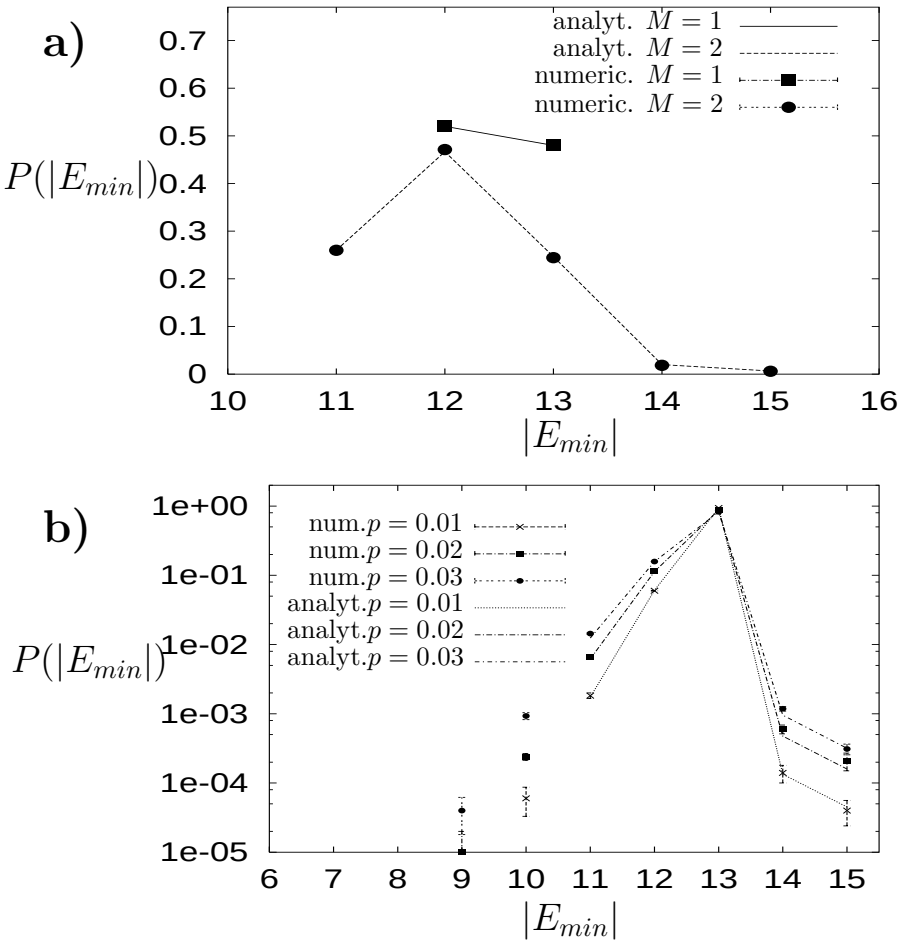
a)
analyt. $M = 1$
analyt. $M = 2$
numeric. $M = 1$
numeric. $M = 2$
$P(|E_{min}|)$
0.7
0.6
0.5
0.4
0.3
0.2
0.1
0
10
11
12
13
14
15
16
$|E_{min}|$
b)
num.$p = 0.01$
num.$p = 0.02$
num.$p = 0.03$
analyt.$p = 0.01$
analyt.$p = 0.02$
analyt.$p = 0.03$
$P(|E_{min}|)$
1e+00
1e-01
1e-02
1e-03
1e-04
1e-05
6
7
8
9
10
11
12
13
14
15
$|E_{min}|$

FIG. 12.